Unfortunately, in the present system, while reaction schemes involving radical intermediates are well precendented for stoichiometric reactions and wholly consistent with all of the available data for this catalytic system, the definitive experiments to test this postulate are inaccessible. The rigorous experimental conditions tend to preclude the use of radical initiators or inhibitors. Similarly, the efficiency of the hydrocarboxylation chemistry involved rules out the use of substrates whose radical derivatives rearrange at near diffusion-controlled bimolecular reaction rates, since such precursors generally contain and take advantage of internal olefinic moieties, which would be preferentially consumed. To avoid these problems and determine more directly the possible intermediacy of radicals, future work will focus on the stoichiometric reaction between $RhI_2(CO)_2^-$ and *i*-PrI (and other secondary iodides) under milder conditions.

(22) Kochi, J. K. "Organometallic Mechanisms and Catalysis"; Academic Press: New York, 1978; p 150.

Acknowledgment. We acknowledge help from R. C. Scheibel with obtaining the mass spectra and also assistance from J. T. Scanlon in setting up the gas chromatographic methods. We also had very useful discussions with Professors R. Grubbs and J. Halpern.

Registry No. *i*-PrOH, 67-63-0; HI, 10034-85-2; *n*-butyric acid, 107-92-6; isobutyric acid, 79-31-2; rhodium, 7440-16-6; deuterium, 7782-39-0.

Supplementary Material Available: Tables I–IV, listing rate data as a function of experimental condition, and Table V, summarizing the analyses of the deuteration studies (12 pages). Ordering information is given on any current masthead page.

Effect of Aryloxide Ancillary Ligands on the Chemistry of Molybdenum–Molybdenum and Tungsten–Tungsten Multiple Metal–Metal Bonds[†1]

Timothy W. Coffindaffer,[‡] Gerald P. Niccolai,[‡] Douglas Powell,[‡] Ian P. Rothwell,*[‡] and John C. Huffman[§]

Contribution from the Chemistry Department, Purdue University, West Lafayette, Indiana 49707, and Molecular Structure Center, Indiana University, Bloomington, Indiana 47405. *Received August 29, 1984*

Abstract: The effect of aryloxide ancillary ligands on the chemistry of Mo_2 and W_2 dinuclear compounds has been investigated by reaction of the compounds $M_2(NMe_2)_6$ (M = Mo and W) and $Mo_2(O\text{-}t\text{-}Pr)_6$ with a variety of phenols. The sterically less demanding ligands 4-methylphenol (HOAr-4-Me) and 3,5-dimethylphenol (HOAr-3,5-Me_2) react with $Mo_2(NMe_2)_6$ to give salt complexes $[Me_2NH_2][Mo_2(OAr)_7(HNMe_2)_2]$ in good yields. A single-crystal diffraction study shows the anion obtained by using 4-methylphenol to contain a confacial bioctahedral arrangement of ligands in the $Mo_2O_7N_2$ core, with a metal–metal distance of 2.601 Å. Both complexes are slightly paramagnetic in solution at 30 °C, μ = 0.8–0.9 μ_B by Evans' method. However, relatively sharp contact shifted ^1H NMR spectra are present at 30 °C for both complexes, and in the case of the 4-methylphenoxo derivative, the temperature dependence of the 4-methyl groups indicates that the electrons on the molybdenum atoms are antiferromagnetically coupled. An estimate of the exchange integral, *J*, gave a value between 230 and 290 cm^{-1}. Using $W_2(NMe_2)_6$ instead of $Mo_2(NMe_2)_6$ in the reaction yields only the simple amine adducts $W_2(OAr\text{-}4\text{-}Me)_6(HNMe_2)_2$ and $W_2(OAr\text{-}3,5\text{-}Me_2)_6(HNMe_2)_2$. Addition of only 4 equiv of 3,5-dimethylphenol to $Mo_2(NMe_2)_6$ in the presence of a large excess of $HNMe_2$ leads to the formation of a reduced, Mo_2^{4+}-containing species $Mo_2(OAr\text{-}3,5\text{-}Me_2)_4(HNMe_2)_4$ as a blue crystalline solid in good yield. Ligand exchange with trimethylphosphine gives the emerald green $Mo_2(OAr\text{-}3,5\text{-}Me_2)_4(PMe_3)_4$. The pathway of the reduction is uncertain, but from the reaction mixture an oxidized species $Mo_2(OAr\text{-}3,5\text{-}Me_2)_6(NMe_2)(HNMe_2)_2$ was isolated and structurally characterized. The Mo_2^{7+} core is surrounded by a confacial bioctahedral arrangement of ligands with a bridging dimethylamido group. The Mo–Mo distance of 2.41 Å is consistent with the presence of a bond of order 2.5. Electrochemical one-electron oxidation of the quadruply bonded $Mo_2(OAr\text{-}3,5\text{-}Me_2)_4(PMe_3)_4$ leads to the monocation containing an Mo_2^{5+} core with a formal bond order of 3.5. EPR measurements show the resulting unpaired electron coupled to the four PMe_3 nuclei. Crystal data for $[Mo_2(OAr\text{-}4\text{-}Me)_7(HNMe_2)_2]\cdot n$-hexane at −163 °C are as follows: a = 14.677 (6) Å, b = 16.62 (7) Å, c = 14.402 (6) Å, α = 115.78 (2)°, β = 107.67 (2)°, γ = 77.82 (2)°, Z = 2, d_{calcd} = 1.281 g cm^{-3} in space group $P\bar{1}$. Crystal data for $Mo_2(OAr\text{-}3,5\text{-}Me_2)_6(NMe_2)(HNMe_2)_2$ at −140 °C are as follows: 29.281 (6) Å, b = 12.071 (4) Å, c = 14.653 (8) Å, β = 92.57 (3)°, Z = 4, d_{calcd} = 1.350 g cm^{-3} in space group $P2_1/n$.

Over the past 20 years, the study of multiple metal–metal bonding has developed rapidly and is presently an important area of inorganic chemistry.[2] Initial endeavers centered mainly on the isolation and characterization of compounds that contained strong metal–metal interactions, but more recently the potential uses of these highly reactive functional groups has been a major focus of research.[3,4] Catalytic cycles in which the electrons initially contained in the metal–metal bond are used have been proposed and, in at least one case, realized.[5] Another major aspect

[†] In this paper the periodic group notation is in accord with recent actions by IUPAC and ACS nomenclature committees. A and B notation is eliminated because of wide confusion. Groups IA and IIA become groups 1 and 2. The d-transition elements comprise groups 3 through 12, and the p-block elements comprise groups 13 through 18. (Note that the former Roman number designation is prevented in the last digit of the numbering: e.g., III → 3 and 13.)

[‡] Chemistry Department.
[§] Molecular Structure Center.

(1) Dinuclear Aryloxide Chemistry, 4. For part 3 see: Coffindaffer, T. W.; Rothwell, I. P.; Huffman, J. C. *Inorg. Chem.*, in press.
(2) Cotton, F. A.; Walton, R. A. "Multiple Bonds Between Metal Atoms"; Wiley: New York, 1982.
(3) Chisholm, M. H.; Rothwell, I. P. *Prog. Inorg. Chem.* **1982**, *29*, 1.
(4) Chisholm, M. H., Ed. *ACS Symp. Ser.* **1981**, *No. 155*, 1.
(5) Chisholm, M. H.; Folting, K.; Huffman, J. C.; Rothwell, I. P. *J. Am. Chem. Soc.* **1982**, *104*, 4389.

0002-7863/85/1507-3572$01.50/0 © 1985 American Chemical Society

of the study of metal–metal bonding is the interrelationship of the sometimes large number of structural types that can exist around a given dimetal center and also the interconversion of metal–metal bonds of different order.[2,3]

This paper deals with the effect that aryloxide ancillary ligands have on the stability, structure, and reactivity of dimolybdenum or ditungsten metal centers. The use of these ligands generates some unusual and unexpected aspects of the chemistry of these dimetal systems and has allowed us to isolate and/or study compounds containing metal–metal bonds of order 2.5, 3.0, 3.5, and 4.0 as well as temperature-dependent metal–metal interaction.[6]

Results and Discussion

The synthetic strategy used for the introduction of aryloxide ligands onto the dimolybdenum and ditungsten centers was simple displacement of dimethylamine or isopropyl alcohol from the basic "Chisholm-type" compounds $M_2(NMe_2)_6$ (M = Mo and W)[7,8] or $Mo_2(O\text{-}i\text{-}Pr)_6$[9] which are considered to contain metal–metal triple bonds with a $\sigma^2\pi^4$ configuration, by addition of the parent phenol. With the sterically demanding 2,6-dimethyl- and 2-*tert*-butyl-6-methylphenol, the extent of substitution depends on the size of the aryloxide ligand, and in some cases only partial substitution occurs.[1,10,11] By this method, we have been totally

$$Mo_2(NMe_2)_6 + 4HOAr\text{-}2,6\text{-}Me_2 \rightarrow Mo_2(OAr\text{-}2,6\text{-}Me_2)_4(NMe_2)_2 + 4HNMe_2$$

$$Mo_2(NMe_2)_6 + \text{xs } HOAr\text{-}2,6\text{-}Me\text{-}t\text{-}Bu \rightarrow Mo_2(OAr\text{-}2,6\text{-}Me\text{-}t\text{-}Bu)_2(NMe_2)_4 + 2\ HNMe_2$$

unable to introduce the extremely bulky 2,6-di-*tert*-butylphenoxide onto these dimetal centers. The structural properties and fluxional behavior of these simple substitution products has been discussed.[10,11] On moving to less sterically demanding phenols, we obtain chemistry significantly different from these simple exchange reactions and totally different from reactivity associated with aliphatic alcohols.[12]

Synthesis of $[Mo_2(OAr)_7L_2]^-$ Derivatives. Addition of 6 or greater equiv of 4-methylphenol (HOAr-4-Me) or 3,5-dimethylphenol (HOAr-3,5-Me_2) to hydrocarbon solutions of $Mo_2(NMe_2)_6$ results in the formation of dark solutions from which over a period of time black crystals precipitate out. Structural studies (vide infra) and microanalytical data are consistent with the formulations $[Me_2NH_2]^+[Mo_2(OAr\text{-}4\text{-}Me)_7(Me_2NH)_2]\cdot C_6H_{14}$ (**1**) and $[Me_2NH_2]^+[Mo_2(OAr\text{-}3,5\text{-}Me_2)_7(Me_2NH)_2]^-$ (**2**). Yields as high as 85% of these compounds can be achieved if between 7 and 10 equiv of parent phenol is used. In terms of reaction stoichiometry, these products can be explained as shown.

$$Mo_2(NMe_2)_6 + 7HOAr \rightarrow [Me_2NH_2][Mo_2(OAr)_7(Me_2NH)_2] + 3Me_2NH$$

No analogous product has been observed with the more bulky 2,6-dimethylphenol. Heating $Mo_2(NMe_2)_6$ with molten, excess HOAr-2,6-Me_2 results only in the formation of deep-red $Mo_2(OAr\text{-}2,6\text{-}Me_2)_6$.[10] Presumably, formation of the anionic complex can be sterically inhibited.

Solid-State Structure of $[Me_2NH_2]^+[Mo_2(OAr\text{-}4\text{-}Me)_7(Me_2NH)_2]\cdot C_6H_{14}$ (1). In order to more fully study the molecular structures of these salts, a single-crystal X-ray diffraction study was carried out on the material obtained from 4-methylphenol

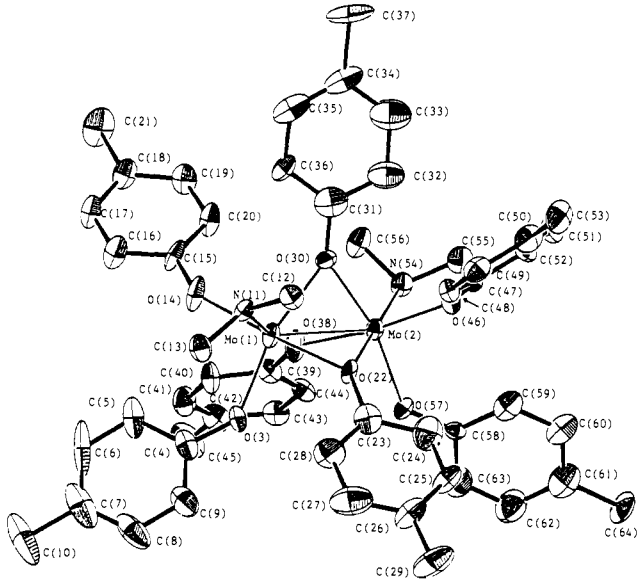

Figure 1. ORTEP view of the anion in $[Me_2NH_2][Mo_2(OAr\text{-}4\text{-}Me)_7(HNMe_2)_2]\cdot n\text{-}C_6H_{14}$ (**1**).

Table I. Crystallographic Data for Compounds **1** and **9**

	1	**9**
formula	$Mo_2O_7N_3C_{61}H_{79}$	$Mo_2O_6N_3C_{54}H_{74}$
mol wt	1158.19	1053.09
space group	$P\bar{1}$	$P2_1/n$
a, Å	14.677 (6)	29.281 (6)
b, Å	16.627 (7)	12.071 (4)
c, Å	14.402 (6)	14.653 (8)
α, deg	115.78 (2)	
β, deg	107.67 (2)	92.57 (3)
γ, deg	77.82	
Z	2	4
V, Å^3	3002.6	5173.9
density (calcd), g/cm^3	1.281	1.350
crystal size, mm	0.21 × 0.23 × 0.19	0.30 × 0.50 × 0.55
crystal color	black	blue
radiation	Mo Kα (λ = 0.71069 Å)	
linear abs coeff, cm^{-1}	4.559	5.2
detector aperture	3.0 mm wide × 4.0 mm high 22.5 cm from crystal	4.0 mm wide × 4.0 mm high 21.0 cm from crystal
sample to source distance	23.5 cm	
takeoff angle, deg	2.0	5.0
scan speed, deg/min	4.0	2–3
scan width, deg	2.0 + 0.692 tan θ	0.9 ± 0.200 tan θ
bkgd counts, s	3	
2θ range, deg	6–45	5–50
data collected	8016	9113
unique data	6714	9106
unique data with $F_o > 2.33\sigma(F)$	5560	6859
$R(F)$	0.073	0.053
$R_w(F)$	0.0678	0.059
goodness of fit	1.365	
largest Δ/σ	0.05	0.06

(**1**). Figure 1 shows an ORTEP view of the anion contained in compound **1**, while Table I contains the crystallographic data and Tables II and III contain the fractional coordinates and some selected bond distances and angles. Views of the $Me_2NH_2^+$ cation and *n*-hexane of crystallization are given in the supplementary material.

As can be seen from Figures 1 and 2, the anion is best described as containing a confacial bioctahedral arrangement of ligands about the two molybdenum atoms. Three aryloxide oxygen atoms lie in bridging positions while each metal contains two terminal aryloxides and one terminal dimethylamine group. The ar-

(6) Coffindaffer, T. W.; Rothwell, I. P.; Huffman, J. C. *Inorg. Chem.* **1983**, *22*, 3187.
(7) Chisholm, M. H.; Cotton, F. A.; Frenz, B. A.; Reichart, W. W.; Shire, L. W.; Stultz, B. R. *J. Am. Chem. Soc.* **1976**, *98*, 4469.
(8) Chisholm, M. H., Cotton, F. A.; Extine, M.; Stultz, B. R. *J. Am. Chem. Soc.* **1976**, *98*, 4477.
(9) Chisholm, M. H.; Reichert, W. W.; Cotton, F. A.; Murillo, C. A. *J. Am. Chem. Soc.* **1977**, *99*, 1652.
(10) Coffindaffer, T. W.; Rothwell, I. P.; Huffman, J. C. *Inorg. Chem.* **1983**, *22*, 2906.
(11) Coffindaffer, T. W.; Rothwell, I. P.; Huffman, J. C. *Inorg. Chem.* **1984**, *23*, 1433.
(12) Chisholm, M. H. *Trans. Met. Chem.* **1978**, *3*, 321.

Table II. Fractional Coordinates and Isotropic Thermal Parameters for $[Me_2NH_2][Mo_2(OAr\text{-}4\text{-}Me)_7(HNMe_2)_2]\cdot n\text{-}C_6H_{14}$ (**1**)

atom	10^4x	10^4y	10^4z	$10B_{iso}$
Mo(1)	8377 (1)	2597 (1)	201 (1)	18
Mo(2)	8627 (1)	2346 (1)	−1622 (1)	16
O(3)	6987 (4)	3025 (4)	328 (5)	23
C(4)	6506 (8)	3416 (6)	1094 (8)	27
C(5)	6915 (9)	3951 (7)	2151 (8)	37
C(6)	6348 (13)	4338 (8)	2892 (9)	60
C(7)	5395 (12)	4173 (9)	2622 (12)	58
C(8)	5016 (10)	3621 (10)	1584 (12)	58
C(9)	5557 (8)	3260 (8)	845 (9)	42
C(10)	4781 (13)	4585 (10)	3472 (13)	79
N(11)	8632 (5)	1581 (5)	893 (6)	19
C(12)	8840 (7)	635 (6)	187 (8)	25
C(13)	7947 (7)	1638 (6)	1486 (8)	27
O(14)	9001 (5)	3358 (4)	1724 (5)	32
C(15)	9657 (8)	3975 (6)	2256 (7)	27
C(16)	9659 (8)	4524 (7)	3302 (8)	34
C(17)	10348 (8)	5140 (7)	3922 (8)	32
C(18)	11048 (8)	5215 (6)	3500 (8)	30
C(19)	11011 (8)	4664 (7)	2435 (8)	29
C(20)	10323 (8)	4059 (6)	1804 (7)	28
C(21)	11834 (9)	5833 (7)	4173 (9)	45
O(22)	7823 (4)	1629 (4)	−1319 (4)	18
C(23)	7025 (6)	1177 (6)	−1866 (7)	34
C(24)	6849 (7)	728 (6)	−2988 (8)	43
C(25)	6068 (7)	219 (6)	−3541 (8)	28
C(26)	5449 (8)	149 (7)	−3047 (9)	34
C(27)	5596 (7)	620 (7)	−1954 (9)	53
C(28)	6390 (7)	1119 (7)	−1357 (7)	40
C(29)	4623 (9)	−459 (10)	−3671 (11)	57
O(30)	9666 (4)	2114 (4)	−359 (5)	21
C(31)	10594 (7)	1793 (6)	−114 (8)	40
C(32)	11096 (7)	1361 (7)	−930 (8)	43
C(33)	12070 (7)	1059 (7)	−667 (9)	51
C(34)	12560 (8)	1169 (7)	353 (10)	37
C(35)	12046 (8)	1571 (8)	1116 (10)	38
C(36)	11092 (7)	1883 (7)	915 (7)	26
C(37)	13620 (8)	860 (9)	601 (12)	53
O(38)	8337 (5)	3567 (4)	−365 (5)	27
C(39)	7975 (7)	4448 (6)	−103 (8)	22
C(40)	7815 (8)	4962 (6)	892 (7)	25
C(41)	7471 (8)	5855 (7)	1167 (8)	31
C(42)	7298 (7)	6266 (6)	472 (9)	30
C(43)	7431 (7)	5744 (6)	−544 (8)	25
C(44)	7761 (7)	4829 (6)	−844 (8)	22
C(45)	6974 (9)	7265 (7)	791 (10)	42
O(46)	9085 (4)	1239 (4)	−2766 (5)	18
C(47)	9373 (6)	380 (6)	−2997 (7)	19
C(48)	9922 (6)	−66 (6)	−3740 (7)	21
C(49)	10231 (7)	−947 (7)	−4037 (8)	32
C(50)	9995 (8)	−1471 (7)	−3616 (9)	34
C(51)	9445 (7)	−1046 (7)	−2882 (8)	29
C(52)	9137 (7)	−133 (6)	−2561 (7)	21
C(53)	10309 (9)	−2470 (7)	−3968 (9)	40
N(54)	9491 (5)	3142 (5)	−1928 (6)	23
C(55)	9953 (7)	2681 (7)	−2814 (8)	29
C(56)	10170 (8)	3692 (7)	−975 (8)	30
O(57)	7419 (4)	2733 (4)	−2582 (4)	18
C(58)	7124 (6)	2568 (6)	−3615 (7)	17
C(59)	7558 (6)	1885 (6)	−4391 (7)	36
C(60)	7248 (7)	1739 (6)	−5464 (7)	39
C(61)	6459 (7)	2269 (6)	−5819 (8)	43
C(62)	6021 (7)	2945 (7)	−5046 (8)	47
C(63)	6647 (7)	3100 (6)	−3963 (8)	41
C(64)	6105 (8)	2115 (8)	−6991 (8)	38
N(65)	5939 (5)	3253 (5)	8447 (7)	44
C(66)	5169 (7)	2679 (7)	7654 (9)	31
C(67)	5551 (8)	4213 (7)	8890 (9)	34
C(68)	2219 (12)	965 (10)	6291 (14)	77
C(69)	2198 (18)	1737 (15)	6043 (16)	112
C(70)	2629 (13)	1828 (15)	5440 (14)	90
C(71)	2691 (15)	2497 (12)	5138 (11)	86
C(72)	3020 (24)	2581 (20)	4444 (20)	164
C(73)	2982 (16)	3276 (13)	4085 (15)	101

rangement of these dimethylamine ligands is such as to generate an approximate C_2 axis for the anion, resulting in their being four

Table III. Selected Bond Distances and Angles for $[Me_2NH_2][Mo_2(OAr\text{-}4\text{-}Me)_7(HNMe_2)_2]\cdot n\text{-}C_6H_{14}$ (**1**)

Mo(1)–Mo(2)	2.601 (2)	Mo(2)–O(22)	2.089 (6)
Mo(1)–O(3)	2.050 (6)	Mo(2)–O(30)	2.112 (6)
Mo(1)–O(14)	2.026 (6)	Mo(2)–O(38)	2.118 (6)
Mo(1)–O(22)	2.110 (5)	Mo(2)–O(46)	2.016 (6)
Mo(1)–O(30)	2.144 (6)	Mo(2)–O(57)	2.068 (6)
Mo(1)–O(38)	2.085 (6)	Mo(2)–N(54)	2.261 (7)
Mo(1)–N(11)	2.226 (7)		
Mo(1)–Mo(2)–O(22)	52.1 (1)	Mo(2)–Mo(1)–O(3)	113.1 (2)
Mo(1)–Mo(2)–O(30)	52.9 (2)	Mo(2)–Mo(1)–O(14)	133.1 (2)
Mo(1)–Mo(2)–O(38)	51.2 (2)	Mo(2)–Mo(1)–O(22)	51.3 (2)
Mo(1)–Mo(2)–O(46)	131.2 (2)	Mo(2)–Mo(1)–O(30)	51.8 (2)
Mo(1)–Mo(2)–O(57)	113.5 (2)	Mo(2)–Mo(1)–O(38)	52.3 (2)
Mo(1)–Mo(2)–N(54)	127.2 (2)	Mo(2)–Mo(1)–N(11)	127.1 (2)
Mo(1)–O(22)–Mo(2)	76.6 (2)		
Mo(1)–O(30)–Mo(2)	75.4 (2)		
Mo(1)–O(38)–Mo(2)	76.5 (2)		

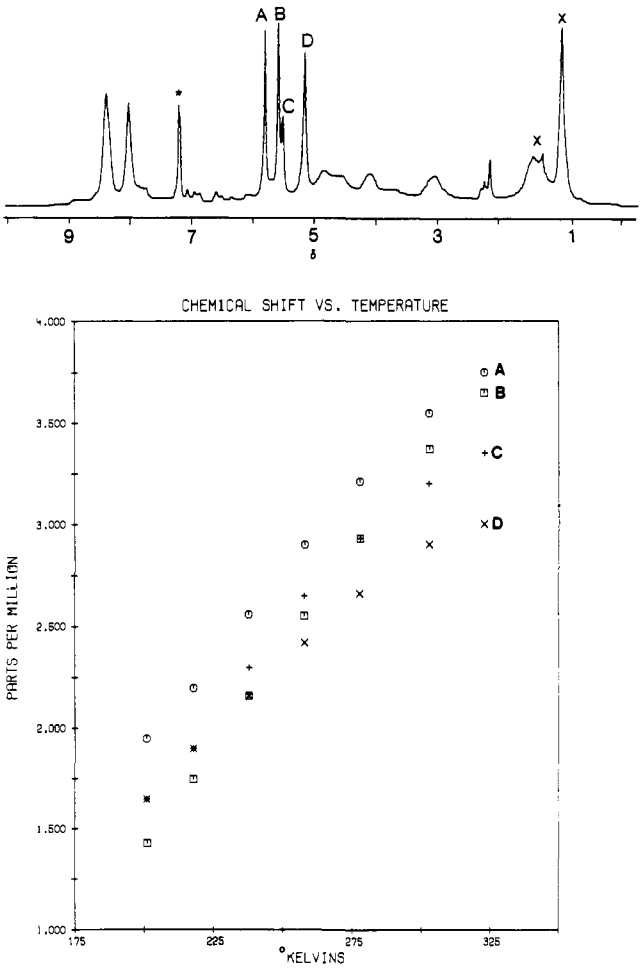

Figure 2. ^1H NMR spectrum (90 MHz) of complex **1** in C_6D_6 and graph showing the temperature dependence of the 4-Me signals with temperature.

types of aryloxide groups in the ratio of 2:2:2:1. The metal–metal distance is 2.601 (2) Å while the Mo–O(bridging) and Mo–O(terminal) distances are 2.11 (av) and 2.03 Å (av). The distances to the terminal Me_2NH are typical for this group attached to molybdenum and are certainly too long for this group to be considered a dimethylamido ligand (NMe_2^-).[13]

The anion in **1** represents an example of a structural type previously only observed with halide ancillary ligands.[2] The "parent" molecules are the series $M_2Cl_9^{3-}$ (M= Cr, Mo, and W), and a number of derivatives of this have been synthesized. For

(13) Chisholm, M. H. *Polyhedron* **1983**, *2*, 681.

the nonahalide, the metal–metal interaction is found to increase as one goes down the triad; in the case of chromium the situation is best represented by two d^3 metals held together by the bridging ligands, while for tungsten a metal–metal triple bond is postulated to account for the observed diamagnetism. In the case of $Mo_2Cl_9^{3-}$, the Mo–Mo distnce is observed to be 2.66 Å and the compound exhibits a temperature-dependent paramagnetism.[14,15] A number of theoretical studies on these molecules have been carried out, and the metal–metal bonding is best described as a strong σ bond and then two weaker bonds that have a mixture of π and δ character with respect to the metal–metal interaction.[16] It is these latter two which are fully developed in the tungsten complex but which for $Mo_2Cl_9^{3-}$ result in the observed temperature-dependent paramagnetism. In the case of compound **1**, the presence of the bridging aryloxide ligands does appear to decrease slightly the metal–metal distance compared to $Mo_2Cl_9^{3-}$, but the complex has comparable magnetic properties (vide infra).

Solution Structure of $[Mo_2(OAr)_7(Me_2NH)_2]^-$ Anions. Both salts exhibit slight paramagnetism in benzene solutions. Measurements by Evans' method (vide infra) indicate a magnetic moment of 0.8–0.9 μ_B at 30 °C. Despite this slight paramagnetism, relatively sharp signals can be observed in the ^1H NMR spectra of both complexes. For the 4-methylphenoxide derivative, a set of well-resolved sharp singlets can be seen in benzene-d_6 or toluene-d_8 solution between δ 5.0 and 6.0 at 30 °C. The intensity ratio of these peaks, 2:2:1:2, leads us to assign them as the 4-methyl resonances of the four types of aryloxide ligands as predicted from the solid-state structure. We hence conclude that the anion is nonfluxional on the NMR time scale at this temperature (Figure 2). The position of these signals is 4 ppm downfield of the normal diamagnetic position of a 4-methyl resonance, implying that they are contact-shifted by the slightly paramagnetic metal center. When these solutions are cooled from +30 to −70 °C, these signals begin to shift upfield toward the "expected" diamagnetic position of *p*-methyl groups at δ 2.0–2.4 ppm (Figure 2). On raising the temperature to +50 °C, they move further downfield. In the case of the 3,5-dimethylphenoxide complex, a similar pattern is evident, but this time much broader and approximately 0.5–1.0 ppm *upfield* of the expected diamagnetic position. When the complex cools, these the signals move downfield. The change in direction of the contact shift of methyl groups on going from the 4- to the 3,5-positions is consistent with the spin density from the metal being transferred through the aromatic ring of the phenoxides to the methyl hydrogen atoms by a hyperconjugative mechanism.[17] This implies that a positive spin density is present at the 4-positions and a negative spin density at the 3,5-positions for the aryloxide group. The chemical shift change on cooling of these resonances is indicative of a diamagnetic–paramagnetic thermal equilibrium for these molecules. Solid-state magnetic measurements on various cation derivatives of $Mo_2Cl_9^{3-}$ have indicated that at room temperature (≈300 K), magnetic moments of 0.5–1.0 μ_B are observed which decrease with decreasing temperature, the solids essentially becoming diamagnetic at low temperatures.[15,18]

Quantitative evaluation of the temperature-dependent chemical shifts observed for complex **1** is not straightforward. The temperature variation of the magnetic susceptibilities of a number of $Mo_2Cl_9^{3-}$ salts has been interpreted in terms of the antiferromagnetic coupling of the three unpaired electrons on each Mo(III) center.[18] In general, the Hamiltonian for exchange coupling of two metal atoms with spins S_1 and S_2 is given by $-2JS_1 \cdot S_2$ where J is the exchange integral of coupling constant and $2J$ represents the separation of the singlet and triplet states. When this model is used, the temperature dependence of the magnetic susceptibilities is fitted to the Van Vleck equation, allowing values of J and g to be obtained.[19] Besides the "classical" case of two Cu(II)-d^9 metal centers interacting,[20] this model has also been applied to a number of other exchange coupled ions including $S = 1$, V(II);[21] $S = {}^3/_2$, Cr,[22] Mo(III),[23] and $S = {}^5/_2$, *Fe*(III).[24]

$$\chi_M = \frac{Ng^2\beta^2}{kT} \frac{\sum(S^2...(-S)^2)e^{-S(S+1)J/kT}}{\sum(2S+1)e^{-S(S+1)J/kT}}$$

The theory of contact shifts when applied to such systems leads to an equation for the temperature dependence very similar to that for magnetic susceptibilities.[24,25] In fact the simple theory predicts superimposable temperature dependencies of χ and $\Delta\nu/\nu_0$. This model has been applied to the contact shifts observed in high-spin bis(iron(III) porphyrin) complexes with $S = {}^5/_2$. Where the value of J and the hyperfine coupling constant A were determined.[26]

Application of these theories to the data obtained on the monoanion **1** requires a number of considerations. First, what diamagnetic value of the chemical shifts of a *p*-cresol methyl group should be used to calculate $\Delta\nu/\nu_0$. To date we have synthesized a number of early transition-metal complexes containing this ligand and find that the 4-methyl resonance always lies between δ 2.05 2.30 ppm in toluene solvent. However, this value is for terminal OAr groups. The effect that bridging two metals has on this group is not presently known, although we believe that the methyl group is sufficiently removed from the metal centers to effectively "buffer" it from such changes. For the purposes of carrying out approximate calculations, we have examined three possible diamagnetic positions of this group at δ 2.0, 2.2, and 2.4 ppm. The second consideration is the possible contribution of pseudocontact shifts (dipolar interactions) to the observed downfield shift of the 4-methyl protons.[27] This contribution is not easy to evaluate even given the structural data available on the complex (**1**). However, we can make a qualitative argument to at least rule out the dominance of dipolar shifts with some confidence. This argument is based on the fact that when the methyl groups of the aryloxide ligands are moved from the 4- to the 3,5-positions, their isotropic shifts move from being negative to positive, consistent with a contact shift mechanism transmitted through the aromatic ring. It is unlikely that a sign change in the geometric factors of the dipolar shift of the methyl groups will occur for this small movement. Similar arguments have been used for other systems.[27]

We can hence go ahead and try to obtain values of J and A from the NMR data assuming only a contract shift contribution. For the purposes of this treatment we have assumed that two of the electrons in the d^3–d^3 dimer are strongly coupled in a σ bond and hence consider the interaction of two $S = 1$ metal centers antiferromagnetically coupled, giving the expression

$$\frac{\Delta\nu}{\nu_0} = \frac{-g\beta}{(\gamma_H/2\pi)3kT} A \frac{(6e^{-2J/kT} + 30e^{-6J/kT})}{(1 + 3e^{-2J/kT} + 5e^{-6J/kT})}$$

In fact, using $S = {}^3/_2$ will give almost identical results at the temperatures concerned due to the negligible contribution that the higher levels of the spin manifold will have in the Boltzmann term.

A brief examination of the data in Figure 2 indicates that for a common diamgnetic position, the four sets of data cannot be fitted with an identical value of J. The four types of methyl groups when fitted to the equation assuming a diamagnetic position of 2.2 give the following values of J (cm^{-1}) and A (Hz); methyl group

(14) Saillant, R. B.; Jackson, R. B.; Streib, W. E.; Folting, K.; Wentworth, R. A. D. *Inorg. Chem.* **1971**, *10*, 1453.
(15) Delphin, W. H.; Wentworth, R. A. D.; Matson, M. S. *Inorg. Chem.* **1974**, *13*, 2552.
(16) Trogler, W. C. *Inorg. Chem.* **1980**, *19*, 697.
(17) Delphin, W. H.; Wentworth, R. A. D. *Inorg. Chem.* **1969**, *8*, 1226.
(18) Grey, E. I.; Smith, P. W. *Aust. J. Chem.* **1969**, *22*, 121.
(19) Van Vleck, J. H. "The Theory of Electric and Magnetic Susceptibilities"; Oxford University Press: London, 1932.
(20) Hodgson, D. J. *Prog. Inorg. Chem.* **1975**, *19*, 173.
(21) Shepherd, R. E.; Hatfield, W. E.; Ghosh, D.; Stout, C. V.; Kristine, F. J.; Ruble, J. R. *J. Am. Chem. Soc.* **1981**, *103*, 5511.
(22) Hatfield, W. E.; MacDougal, J. J.; Shepherd, R. E. *Inorg. Chem.* **1981**, *20*, 4216.
(23) Earnshaw, A.; Lewis, J. *J. Chem. Soc. A* **1961**, 396.
(24) Fleischer, E. B., Palmer, J. M.; Srivastava, T. S.; Chatterjee, A. *J. Am. Chem. Soc.* **1971**, *93*, 3162.
(25) Holm, R. H.; Hawkins, C. J. In "NMR of Paramagnetic Molecules"; LaMar, G. N., Horrocks, W. D., Holm, R. H., Eds.; Academic Press, New York, 1973; Chapter 7.
(26) Boyd, P. D. W.; Smith, T. D. *Inorg. Chem.* **1971**, *10*, 2041.
(27) Horrock, W. D., ref 25, Chapter 4.

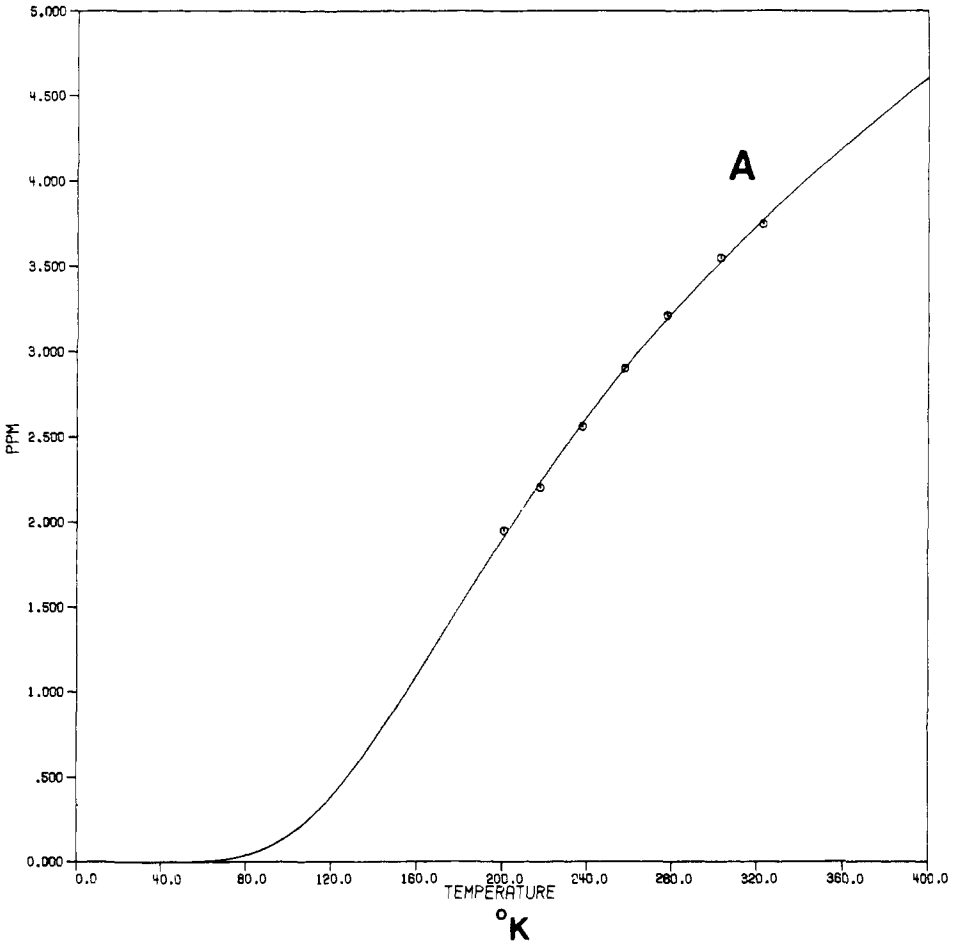

Figure 3. Plot showing the fitting of the temperature dependence of the chemical shift of methyl group A. The curve is obtained by using $J = -229$ cm^{-1}; $A_1 = 1.76 \times 10^5$ Hz; $A_2 = 3.62 \times 10^5$ Hz.

(A), −241, 2.11×10^5; (B), −287, 2.94×10^5; (C), −249, 2.03×10^5; (D), −229, 1.55×10^5. Clearly there is a problem either with the data or with the model, especially for methyl group B which gives a much larger predicted value of J. A problem with the data may be a large discrepancy in the diamagnetic positions of the four types of methyl groups. If methyl group B had a diamagnetic position only 0.2 ppm upfield of the other three groups, it would bring the predicted value of J for this group down to −273 cm^{-1}. Furthermore, if the other three groups are now assigned a diamagnetic position 0.2 ppm more downfield, then even closer agreement can be obtained. However, we feel that the resulting 0.4 ppm spread of 4-methyl groups would be unprecedented in view of the data we have at present on 4-methylphenoxide derivatives of early transition metals. An obvious possible error is the presence of a small but significant pseudocontact shift contributing nonequivalently to each of the 4-methyl groups.

In terms of the theoretical treament of the data, an assumption implicit in eq 2 is that the hyperfine coupling constant, A, is the same for both the excited states of the spin manifold.[25] There is no reason to assume in fact that this is the case, and a more general expression would be

$$\frac{\Delta\nu}{\nu_0} = \frac{-g\beta}{(\gamma_H/2\pi)3kT} \frac{(A_1 6e^{-2J/kT} + A_2 30e^{-6J/kT})}{(1 + 3e^{-2J/kT} + 5e^{-6J/kT})}$$

Analysis of this equation for the temperature and magnitude of J we have in this system shows that at 201 K, only a negligible contribution will be made by A_2 assuming $A_2 < 100A_1$. However, at 320 K, if A_2 is only $2A_1$, it can make a considerable difference. If $A_2 < A_1$, it will make little difference to the results obtained with the simpler model. When this model is used, all the data can be fit to a single value of J, but the resulting fit with the experimental data is very poor. However, fitting the four sets of data independently to J, A_1, and A_2 yields slightly better fits but again a range of J values (Figure 3).

Taking these calculated values of J, one can now estimate an expected magnetic moment for the complex at 30 °C. When eq 1 is used and $g = 2$ is assumed, then a value of $\mu_{obsd} = 1.2$–1.3 μ_B is expected. Solution measurements on both salt complexes by Evans' method[28] gave solution magnetic moments of 0.87 μ_B (benzene), 0.85 μ_β (toluene) for the 4-methyl complex **1**, and 0.88 μ_B (toluene) for the 3,5-dimethyl salt **2**. We hence conclude that the temperature dependence of the ^{1}H NMR signals in these complexes allows a reasonable estimate of the magnitude of the metal–metal interaction in solution.

Pathway for Formation of $[Mo_2(OAr)_7(HNMe_2)_2]^-$. The formation of the $Mo_2(OAr)_7L_2^-$ anions represents the first example of the direct interconversion of a "Chisholm-type" compound, M_2X_6 with a strong, unbridged metal–metal triple bond, to a compelx $X_3M(\mu\text{-}X)_3MX_3$ with a confacial bioctahedral geometry and significantly less metal–metal interaction.

The question arises to whether one can identify the intermediate steps leading to these anionic species. Stoichiometrically one can consider them as arising by addition of aryloxide anion (OAr^-) to a complex of formula $Mo_2(OAr)_6(HNMe_2)_2$. The elegant reaction schemes worked out by Chisholm et al. for the analogous alkoxide chemistry show that treatment of $Mo_2(NMe_2)_6$ with alcohols (excess) can lead to the hexaalkoxides $Mo_2(OR)_6$ containing the unbridged, ethane-like structure typical of the Mo_2^{+6} derivatives.[9] The complexes $Mo_2(OR)_6$ will readily "pick up" neutral donor ligands (such as $HNMe_2$) to form the complexes $Mo_2(OR)_6(L)_2$ (L = donor ligand).[29] Structural studies show that such adducts, still retaining an Mo_2^{+6} core, contain two four-coordinate, unbridged metal centers with a square-planar

(28) Evans, D. F. *J. Chem. Soc.* **1959**, 2003.
(29) Chisholm, M. H.; Cotton, F. A.; Extine, M. W.; Reichert, W. W. *J. Am. Chem. Soc.* **1978**, *100*, 153.

arrangement of the three oxygen atoms and one neutral donor atom.[29] In the case of the ditungsten alkoxide analogues, similar chemistry exists although a complexity arises in some cases because of the possible oxidation that can occur at the W_2^{+6} core by oxidative addition of RO–H bonds.[30] In the case of aryloxides, we have also been able to synthesize direct analogues of these structural types. Hence, by treating $Mo_2(O\text{-}i\text{-}Pr)_6$ with 3,5-dimethylphenol (>6 equiv) in hydrocarbon solvents and removing the more volatile isopropyl alcohol so formed, we have isolated the hexaaryloxide $Mo_2(OAr\text{-}3,5\text{-}Me_2)_6$ (**3**). Addition of 4-fluorophenol (HOAr-4-F) to $Mo_2(NMe_2)_6$ in hexane leads to a precipitate of sparingly soluble $Mo_2(OAr\text{-}4\text{-}F)_6(HNMe_2)_2$ (**4**) as a dark-red solid.

Attempts to synthesize the tungsten analogues of the anionic complexes by addition of HOAr to $W_2(NMe_2)_6$ results only in the formation of the simple amine adducts $W_2(OAr\text{-}4\text{-}Me)_6(HNMe_2)_2$ (**5**) and $W_2(OAr\text{-}3,5\text{-}Me_2)_6(HNMe_2)_2$ (**6**). Hence,

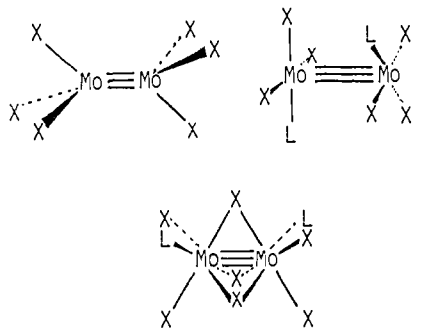

it appears that aryloxide ancillary ligands can support all three of these structural types.

The isolation of the hexaaryloxide $Mo_2(OAr\text{-}3,5\text{-}Me_2)_6$ (**3**) allows one to attempt the formation of the anionic complex **2** by an additional route. Addition of $HOAr\text{-}3,5\text{-}Me_2$ to the parent hexaaryloxide followed by addition of $HNMe_2$ does result in the formation of small amounts of the corresponding salt, but the amount converted is very low. A mixture of other, unidentified products is given. A possible pathway for the formation of the salts **1** and **2** from the parent hexamide would involve the precoordination of HOAr followed by its deprotonation rather than direct attack by OAr^-, an unlikely species under the conditions present. However, bearing in mind the fact that conversion of $Mo_2(OAr)_6$ to $Mo_2(OAr)_7L_2^-$ is not readily achieved may indicate that structural changes to a confacial bioctahedron may be occuring earlier in the reaction, prior to total amide substitution. In order to study the reaction of $Mo_2(NMe_2)_6$ with less sterically bulky aryl alcohols further, we investigated the products obtained when less than 6 equiv of HOAr was used. To our surprise, a totally new reactivity pattern was generated which throws little light on the possible pathway of formation of the heptaphenoxide anions.

Synthesis of $Mo_2(OAr\text{-}3,5\text{-}Me_2)_4(HNMe_2)_4$ (7). Addition of only 4 equiv of 3,5-dimethylphenol ($HOAr\text{-}3,5\text{-}Me_2$) to hexane solutions of $Mo_2(NMe_2)_6$ resulted in a deep-red solution which over a period of hours deposited deep-blue crystals of $Mo_2(OAr\text{-}3,5\text{-}Me_2)_4(HNMe_2)_4$ (**7**) identified by microanalytical data, spectroscopic properties, and chemical reactivity (vide infra). Yields of the order of 15–30% of pure, crystalline material were obtained. However, by condensing into the solution a large excess of dimethylamine, the yield of pure $Mo_2(OAr\text{-}3,5\text{-}Me_2)_4(HNMe_2)_4$ (**7**) was increased to 65%. The deep-blue product is slightly soluble in hexane and moderately soluble in benzene and toluene, giving intense blue solutions. ^1H NMR spectra of **7** in benzene-d_6 show the presence of the aryloxide methyl groups as a singlet at δ 2.3. Slightly downfield of this and of equal intensity is a doublet assignable to the $HN\mathit{Me}_2$ groups of the coordinated dimethylamine. The $\mathit{H}NMe_2$ proton is also present as a moderately well-resolved septet at δ 6.59. The electronic absorption spectrum

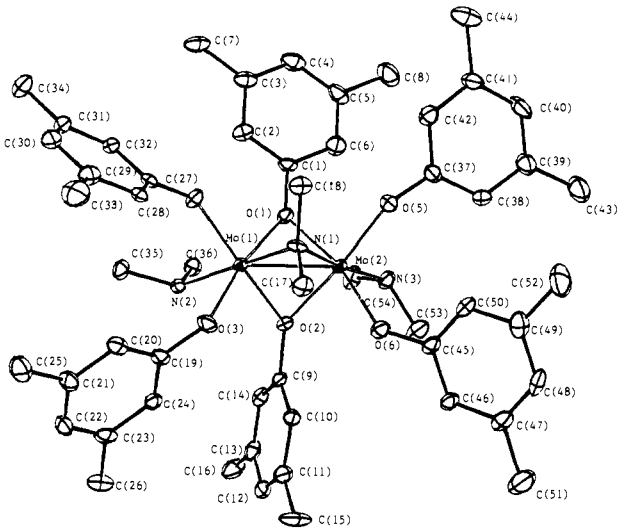

Figure 4. ORTEP view of the molecule $Mo_2(OAr\text{-}3,5\text{-}Me_2)_6(NMe_2)(HNMe_2)_2$ (**9**).

shows a broad band centered at 584 nm assignable to the δ–δ^* transition of the quadruple bond one expects for this Mo_2^{4+}-containing species (Figure 4). Addition of PMe_3 to the tetradimethylamine complex does not result in rapid exchange of PMe_3 for $HNMe_3$. However, on refluxing neat PMe_3 solutions of the complex, the initially blue solution becomes dark green and removal of solvent allows the isolation of pure, green $Mo_2(OAr\text{-}3,5\text{-}Me_2)_4(PMe_3)_4$ (**8**). The presence of coordinated PMe_3 is evident in the ^1H NMR spectrum as an ill-resolved triplet at δ = 1.37, indicative of virtual coupling of the PMe_3 protons of two *trans*-PMe_3 groups. A shift in the visible absorption band from 584 to 673 nm accounts for the change in color from blue to green on ligand substitution (Figure 4). In the ^{31}P NMR spectrum, a singlet resonance is seen at δ −9.87.

Compounds **7** and **8** represent further examples of the general series of complexes $Mo_2X_4L_4$ (X = monoanionic group, L = neutral donor ligand), containing an Mo_2^{4+} core with a $\sigma^2\pi^4\delta^2$ electron configuration, to generate a quadruple metal–metal bond.[2] The earliest, and by far most thoroughly studied, members of this group are the tetrahalo, tetraphosphine complexes $Mo_2X_4(PR_3)_4$ (X Cl, Br, and I). A series of thiocyanate complexes had also been synthesized.[31] More recently, Chisholm and workers reported the synthesis and extensive structural characterization of a number of alkoxy compounds $Mo_2(OR)_4(L)_4$.[32] These compounds containing the Mo_2^{4+} core were obtained by reductive elimination of alkyl ligands from an Mo_2^{6+} core.[33,34]

Structural studies on compounds of this type typically show an unbridged Mo_2^{4+} core with each metal surrounded by an approximately square-planar arrangement of X and L donor atoms. The two square planes are eclipsed as one might expect for the full development of the δ bond. Although two trans isomers are possible, only isomer (a) has been characterized so far for monodentate L. However, the possible intermediate formation

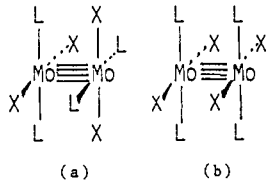

(a) (b)

and subsequent isomerization of a molecule with structure (b) has been proposed.[35] Our attempts to structurally characterize either

(30) Akiyama, M.; Chisholm, M. H.; Cotton, F. A.; Extine, M. W.; Haitko, D. A.; Leonelli, J.; Little, D. *J. Am. Chem. Soc.* **1981**, *103*, 779.

(31) Nimry, T.; Walton, R. A. *Inorg. Chem.* **1978**, *17*, 510.

(32) Chisholm, M. H.; Folting, K.; Huffman, J. C.; Tatz, R. J. *J. Am. Chem. Soc.* **1984**, *106*, 1153.

(33) Chisholm, M. H.; Cotton, F. A.; Extine, M.; Miller, M.; Stultz, B. R. *Inorg. Chem.* **1976**, *15*, 2244.

(34) Chisholm, M. H.; Haitko, D. A. *J. Am. Chem. Soc.* **1979**, *101*, 6784.

7 or **8** by single-crystal X-ray diffraction studies has so far been unsuccessful. However, in view of the large body of data on related complexes, we feel confident that geometrical isomer (a) is present for both of these complexes. The conversion of $Mo_2(NMe_2)_6$ to $Mo_2(OAr\text{-}3,5\text{-}Me_2)_4(HNMe_2)_4$ by simple addition of 4 equiv of phenol under mild conditions is rather a remarkable reaction and again raises the question whether it is possible to more fully understand the reaction and the intermediate steps in the transformation. For instance at what step does reduction take place, and what species is being oxidized? The addition of 4 equiv of phenol should lead, via stepwise substitution, to a molecule of formula $Mo_2(OAr\text{-}3,5\text{-}Me_2)_4(NMe_2)_2$. An analogous compound $Mo_2(OAr\text{-}2,6\text{-}Me_2)_4(NMe_2)_2$, where OAr-2,6-$Me_2$ is the more sterically demanding 2,6-dimethylphenoxide, has been previously synthesized and structurally characterized.[11] This complex exhibits a great deal of thermal stability and shows no tendency to form a reduced complex. We believe that due to the much smaller steric requirements of 3,5-dimethylphenoxide, it is possible at this stage of substitution for dimethylamine to remain coordinated, forming a complex of formula $Mo_2(OAr)_4(NMe_2)_2(HNMe_2)_2$. Absorption of two electrons and two protons now leads to the desired product. The reverse processes, i.e., removal of two electrons and two protons, we believe can be achieved electrochemically (vide infra). We have been unable at present to conclusively identify the chemical source of the electrons for this reduction. Three possibilities seem reasonable.

(i) The increased yield of the quadruply bonded compound **7** on addition of a large excess of dimethylamine could indicate that this molecule is acting as the reducing agent. This idea has a great deal of precedence. It has been shown by Walton and co-workers that $(MoCl_3)_n$ can be reduced with neat $HNMe_2$ to generate the complexes $Mo_2Cl_4(HNMe_2)_4$ in yields of 40–50%.[36] One can, therefore, write a balanced redox reaction as shown below:

$$Mo_2(OAr)_4(NMe_2)_2(HNMe_2)_2 + HNMe_2 \rightarrow Mo_2(OAr)_4(HNMe_2)_4 + CH_2{=}N(CH_3)$$

We have been unable to identify any methylimine spectroscopically in the reaction mixture leading to the Mo_2^{4+} product. It is also possible that the $HNMe_2$ is important in increasing yield not as reducing agent but in order to maintain a high concentration of an intermediate ammine adduct.

(ii) An important and well-studied reaction of phenols is their relative ease of oxidation that can lead either to dimeric or polymeric materials.[37] It is hence feasible that the phenoxo ligands are themselves the reducing agents.

On removing the solvent from the reaction mixture after **7** has been isolated, a brown oil is given. Analysis of this oil by ^1H NMR shows the presence of some of the quadruple-bonded compound along with a complex mixture of other products, none of which we have been able to identify.

(iii) The final possibility is an amine-induced disproportionation reaction of the dimetal center. This can be represented by the balanced equation

$$aMo_2^{6+} \rightarrow bMo_2^{4+} + \left(\frac{6a-4b}{n}\right) Mo_2^{n+}$$

Clearly n must be >6, and the yield of the reaction (>65%) predicts its possible value as 10, i.e., Mo_2^{10+} possibly containing an Mo–Mo single bond. However, it seems reasonable that under the reaction conditions, a mixture of oxidized species may be present, especially in view of the isolation of a small amount of an Mo_2^{7+}-containing compound.

Isolation of $[Mo_2(OAr\text{-}3,5\text{-}Me_2)_6(NMe_2)(HNMe_2)_2]$ (9). As indicated earlier, attempts to obtain a satisfactory single-crystal X-ray diffraction structure of the complexes *7* and *8* were unsuccessful. However, a deep-blue crystal taken from a bulk sample of $Mo_2(OAr\text{-}3,5\text{-}Me_2)_4(HNMe_2)_4$ (**7**) (Figure 5) obtained directly from the reaction mixture was found to contain a new material whose solid-state structure was successfully solved. Structural analysis showed the compound to have a formula $[Mo_2(OAr\text{-}3,5\text{-}Me_2)_6(NMe_2)(HNMe_2)_2]$, indicating an Mo_2^{7+} core.

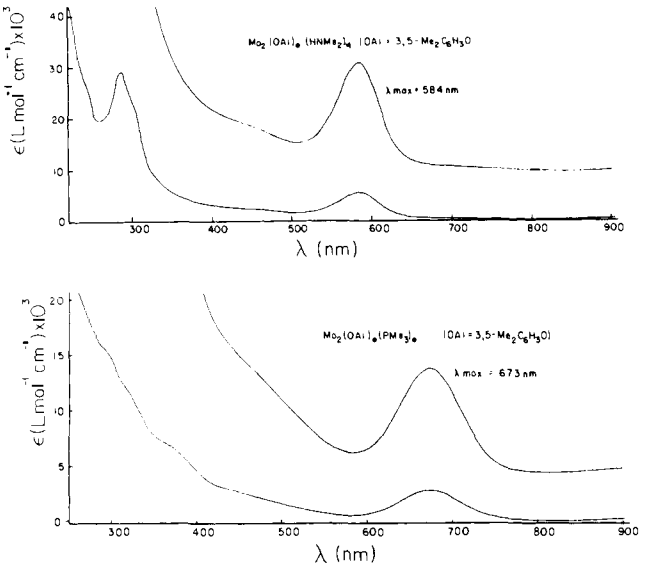

Figure 5. Electronic absorption spectra of complexes $Mo_2(OAr\text{-}3,5\text{-}Me_2)_4(L)_4$ (L = $HNMe_2$, PMe_3) recorded in cyclohexane solvent.

Table I contains the crystallographic data for the complex while Tables IV and V contain fractional coordinates and some important bond distances and angles. A view of the molecule with the numbering scheme is shown in Figure 4. The molecule can be seen to adopt an overall confacial bioctahedral structure analogous to that seen for the $[Mo_2(OAr\text{-}4\text{-}Me)_7(HNMe_2)_2]^-$ anion previously. The two metal centers are bridged by two aryloxide ligands and, rather rarely, a bridging dimethylamido group. The other four aryloxides are terminal with the two terminal dimethylamine ligands situated *trans* to the bridging NMe_2 group. The terminal Mo–OAr distances of 1.96 Å (av) are slightly shorter than the corresponding distances in the monoanion **1**, while bridging Mo–OAr distances of 2.12 Å (av) are comparable. The distances to the bridging NMe_2^- group, 2.11 and 2.12 Å, are shorter than the terminal Mo–$NHMe_2$ distances of 2.26 and 2.29 Å, but significantly longer than typical terminal Mo–NMe_2 distances of 1.90–2.00 Å found for midoxidation state molybdenum.[38] The presence of considerable π interaction between nitrogen p and molybdenum d orbitals is the obvious reason for the shorter terminal values of NMe_2 groups.

The formal oxidation state of the complex implies a Mo_2^{7+} core. Allowing full overlap of metal–metal orbitals, this should result in a bond order of 2.5 with a single unpaired electron. The Mo–Mo bond distance of 2.41 Å is in fact consistent with this picture (vide infra) and contrasts with the distance of 2.60 Å observed previously for the monoanion (**1**). Just as the monoanion could be considered as being a derivative of the trianion $Mo_2Cl_9^{3-}$, so the complex **9** can be considered a derivative of the dianion $Mo_2Cl_9^{2-}$ which has been synthesized by a number of routes including oxidation of $Mo_2Cl_9^{3-}$.[39]

Unfortunately, all attempts at isolating any quantities of **9** have failed, and we believe it is only a minor product from the reaction mixture leading to $Mo_2(OAr\text{-}3,5\text{-}Me_2)_4(HNMe_2)_4$ (**7**) that we have fortuitously crystallized out. Neither this sample of **7** or recrystallized **7** gave an ESR signal. Hence **9** is indeed a very small component of the reaction mixture.

Comparison of the Structures of 1 and 9 with Other Confacial–Bioctahedral Mo_2-Containing Species. The confacial–bioctahedral geometry M_2X_9 is a very common system in inorganic

(35) Carmona-Guzman, E.; Wilkinson, G. *J. Chem. Soc., Dalton Trans.* **1977**, 1716.
(36) Armstrong, J. E.; Edwards, D. A.; Maguire, J. J.; Walton, R. A. *Inorg. Chem.* **1979**, *18*, 1172.
(37) Parshall, G. W. "Homogeneous Catalysis"; Wiley: New York, 1980.
(38) Haymore, B. L.; Nugent, W. A. *Coord. Chem. Rev.* **1980**, *31*, 123.
(39) Delphin, W. H.; Wentworth, R. A. D. *J. Am. Chem. Soc.* **1973**, *95*, 7920.

Table IV. Fractional Coordinates and Isotropic Thermal Parameters for $Mo_2(NMe_2)(OAr\text{-}3,5\text{-}Me_2)_6(HNMe_2)_2$ (**9**)

atom	10^4x	10^4y	10^4z	B, Å^2
Mo1	72188 (2)	2264 (4)	92252 (3)	1.041 (9)
Mo2	64334 (2)	−3721 (4)	92666 (3)	1.124 (9)
O1	6724 (1)	356 (3)	8110 (2)	1.49 (8)
O2	6683 (1)	1157 (3)	9776 (2)	1.27 (8)
O3	7575 (1)	201 (3)	10383 (2)	1.78 (8)
O4	7675 (1)	−343 (3)	8377 (2)	1.59 (8)
O5	6183 (1)	−1645 (3)	8566 (2)	1.70 (8)
O6	6209 (1)	−713 (3)	10475 (2)	1.70 (8)
N1	7013 (2)	−1407 (4)	9504 (3)	1.23 (9)
N2	7491 (2)	1951 (4)	8984 (3)	1.25 (9)
N3	5785 (2)	632 (4)	8917 (3)	1.6 (1)
C1	6683 (2)	180 (5)	7187 (3)	1.5 (1)
C2	7061 (2)	245 (5)	6658 (4)	1.7 (1)
C3	7019 (2)	44 (5)	5716 (4)	1.9 (1)
C4	6595 (2)	−203 (5)	5330 (4)	2.4 (1)
C5	6207 (2)	−252 (5)	5840 (4)	2.1 (1)
C6	6255 (2)	−72 (5)	6785 (4)	2.1 (1)
C7	7436 (2)	81 (5)	5151 (4)	2.3 (1)
C8	5745 (2)	−500 (6)	5402 (4)	3.2 (2)
C9	6664 (2)	1791 (5)	10554 (3)	1.3 (1)
C10	6686 (2)	1319 (5)	11416 (4)	1.5 (1)
C11	6686 (2)	2014 (5)	12181 (4)	1.9 (1)
C12	6666 (2)	3148 (5)	12074 (4)	1.9 (1)
C13	6633 (2)	3624 (5)	11207 (4)	1.7 (1)
C14	6635 (2)	2943 (5)	10452 (4)	1.6 (1)
C15	6718 (3)	1504 (6)	13128 (4)	3.1 (2)
C16	6604 (2)	4862 (5)	11123 (4)	2.6 (1)
C17	7103 (2)	−1871 (5)	10417 (4)	1.7 (1)
C18	7095 (2)	−2262 (5)	8810 (4)	1.9 (1)
C19	7914 (2)	762 (5)	10839 (3)	1.5 (1)
C20	8349 (2)	303 (5)	10935 (4)	1.8 (1)
C21	8696 (2)	837 (5)	11423 (4)	1.9 (1)
C22	8608 (2)	1869 (5)	11806 (4)	2.0 (1)
C23	8182 (2)	2340 (5)	11717 (3)	1.7 (1)
C24	7832 (2)	1792 (5)	11223 (4)	1.6 (1)
C25	9166 (2)	318 (6)	11531 (4)	2.8 (1)
C26	8085 (2)	3449 (5)	12148 (4)	2.6 (1)
C27	8113 (2)	−646 (5)	8325 (4)	1.6 (1)
C28	8326 (2)	−1351 (5)	8960 (4)	1.6 (1)
C29	8783 (2)	−1637 (5)	8888 (4)	2.2 (1)
C30	9018 (2)	−1250 (5)	8151 (4)	2.4 (1)
C31	8812 (2)	−568 (5)	7492 (4)	2.2 (1)
C32	8361 (2)	−278 (5)	7588 (4)	1.8 (1)
C33	9016 (2)	−2356 (6)	9604 (5)	3.1 (2)
C34	9073 (2)	−164 (6)	6690 (5)	3.0 (2)
C35	7987 (2)	2020 (5)	8799 (4)	1.7 (1)
C36	7224 (2)	2594 (5)	8289 (4)	1.7 (1)
C37	5825 (2)	−2044 (5)	8064 (4)	1.6 (1)
C38	5376 (2)	−2003 (5)	8349 (4)	1.9 (1)
C39	5022 (2)	−2475 (5)	7810 (5)	2.7 (1)
C40	5121 (2)	−2977 (5)	6993 (5)	2.7 (1)
C41	5561 (2)	−3040 (5)	6696 (4)	2.2 (1)
C42	5910 (2)	−2562 (5)	7237 (4)	1.9 (1)
C43	4547 (3)	−2479 (7)	8134 (6)	4.4 (2)
C44	5665 (3)	−3579 (6)	5788 (4)	3.5 (2)
C45	5907 (2)	−1346 (5)	10909 (3)	1.5 (1)
C46	5708 (2)	−920 (5)	11679 (4)	1.7 (1)
C47	5401 (2)	−1552 (5)	12163 (4)	2.1 (1)
C48	5297 (2)	−2614 (5)	11859 (4)	2.1 (1)
C49	5491 (2)	−3044 (5)	11085 (4)	2.1 (1)
C50	5795 (2)	−2413 (5)	10616 (4)	1.7 (1)
C51	5187 (2)	−1064 (7)	12997 (4)	3.4 (2)
C52	5355 (2)	−4178 (6)	10741 (5)	3.4 (2)
C53	5501 (2)	832 (6)	9703 (4)	2.4 (1)
C54	5876 (2)	1703 (5)	8466 (4)	2.2 (1)

coordination chemistry. Sometime ago Cotton and Ucko formulated a method of measuring the distortions from pure octrahedral geometries that occur for the metals in such systems and evaluating these distortions in terms of direct metal–metal interactions.[40] In the field of metal–metal multiple-bonded compounds, it is now common for authors to cite that a metal–metal distance lies within the range "expected" for a particular bond order. This degree of certainty is based on the now large body of structural data dealing with metal–metal-bonded compounds and has allowed the range that such distances cover to be quite narrowly defined; see Cotton and Walton, p 340. However, in the case of the cofacial–bioctahedral geometry for the group 6 metals, the difficulty in sometimes obtaining sufficient metal orbital overlap can lead to a very large range of metal–metal distances for an identical M_2^{x+} core. In this geometry, the metal ligation can have a profound effect on the metal–metal distance. Theoretical studies by Hoffman and Summerville have shown that the π-acceptor or -donor properties of ligands directly affect the metal–metal interaction.[41] Table VI contains the structural data for a number of complexes containing an Mo_2 center in a cofacial–bioctahedral arrangement of ligands. Because of the fact that all nine donor atoms are rarely equivalent, the treatment of Cotton and Ucko is no longer valid. However, the effect of the differing ligands on the metal–metal distance is easily assessed.

Table V. Selected Bond Distances and Angles for $Mo_2(NMe_2)(OAr\text{-}3,5\text{-}Me_2)_6(HNMe_2)_2$ (**9**)

Mo(1)–Mo(2)	2.4139 (6)	Mo(2)–O(1)	2.120 (4)
Mo(1)–O(1)	2.140 (3)	Mo(2)–O(2)	2.109 (4)
Mo(1)–O(2)	2.119 (4)	Mo(2)–O(5)	1.971 (4)
Mo(1)–O(3)	1.952 (3)	Mo(2)–O(6)	1.959 (4)
Mo(1)–O(4)	1.987 (4)	Mo(2)–N(1)	2.124 (4)
Mo(1)–N(1)	2.107 (4)	Mo(2)–N(3)	2.290 (5)
Mo(1)–N(2)	2.263 (4)		
Mo(1)–Mo(2)–O(1)	55.9 (1)	Mo(2)–Mo(1)–O(1)	55.1 (1)
Mo(1)–Mo(2)–O(2)	55.4 (1)	Mo(2)–Mo(1)–O(2)	55.0 (1)
Mo(1)–Mo(2)–O(5)	123.6 (1)	Mo(2)–Mo(1)–O(3)	116.5 (1)
Mo(1)–Mo(2)–O(6)	116.4 (1)	Mo(2)–Mo(1)–O(4)	128.4 (2)
Mo(1)–Mo(2)–N(1)	54.9 (1)	Mo(2)–Mo(1)–N(1)	55.5 (1)
Mo(1)–Mo(2)–N(3)	128.1 (1)	Mo(2)–Mo(1)–N(2)	128.5 (1)
Mo(1)–O(1)–Mo(2)	69.0 (2)		
Mo(1)–O(2)–Mo(2)	69.6 (2)		
Mo(1)–N(1)–Mo(2)	69.6 (1)		

Table VI. A Comparison of Some Confacial Bioctahedral Complexes Containing Mo_2 Cores

complex	bridging atoms	max BO	Mo–Mo Dist	ref
$Cs_3Mo_2Cl_9$	Cl_3	3	2.655 (11)	14
$[Me_2NH_2][Mo_2(OAr)_7(HNMe_2)_2]$	O_3	3	2.601 (2)	this work
$[Ph_4P][Mo_2Cl_7(SMe_2)_2]$	Cl_3	3	2.746 (9)	42
$Mo_2Cl_6(SMe_2)_3$	S, Cl_2	3	2.462 (2)	42
$(pyH)_3Mo_2Cl_8H$	H, Cl_2	3	2.371 (1)	43
$Mo_2(O\text{-}i\text{-}Pr)_6(CO)(py)_2$	CO, O_2	2	2.486 (2)	44
$Mo_2(OAr)_6(NMe_2)(HNMe_2)_2$	N, O_2	2.5	2.414 (1)	this work

For the complexes containing an Mo_2^{6+} core, it can be seen that the Mo–Mo distance can vary from 2.82 to 2.38 Å. This distance compares with the 2.20–2.23-Å distance typical of Mo_2X_6. Chisholm-type compounds with an unbridged Mo–Mo triple bond.[2] The total diamagnetic nature of the two complexes with the shortest distances leads one to the conclusion that a fully formed triple bond in such systems should result in a distance of the order of 2.4 Å. Clearly the complex $Mo_2(OAr\text{-}4\text{-}Me)_7(HNMe_2)_2^-$ (**1**) with a distance of 2.60 Å does not have a "fully formed" triple bond, and thermal population of paramagnetic states, i.e., states with decreased Mo–Mo bond order, is possible as discussed earlier. On moving to the neutral complex $Mo_2(OAr\text{-}3,5\text{-}Me_2)_6(NMe_2)(HNMe_2)_2$ (**9**), however, a dramatic decrease in the value of the Mo–Mo distance to 2.41 Å occurs. Both of these complexes have the identical set of terminal ligands, four OAr groups and two $HNMe_2$ molecules. However, instead of having three bridging aryloxides, the neutral molecule has two aryloxides and one dimethylamido ligand. Furthermore, one predicts that there will be one less electron available in the Mo_2^{7+} core for bonding. No

(40) Cotton, F. A.; Ucko, D. A. *Inorg. Chim. Acta* **1972**, *6*, 161.

(41) Summerville, R. H.; Hoffman, R. *J. Am. Chem. Soc.* **1979**, *101*, 3821.

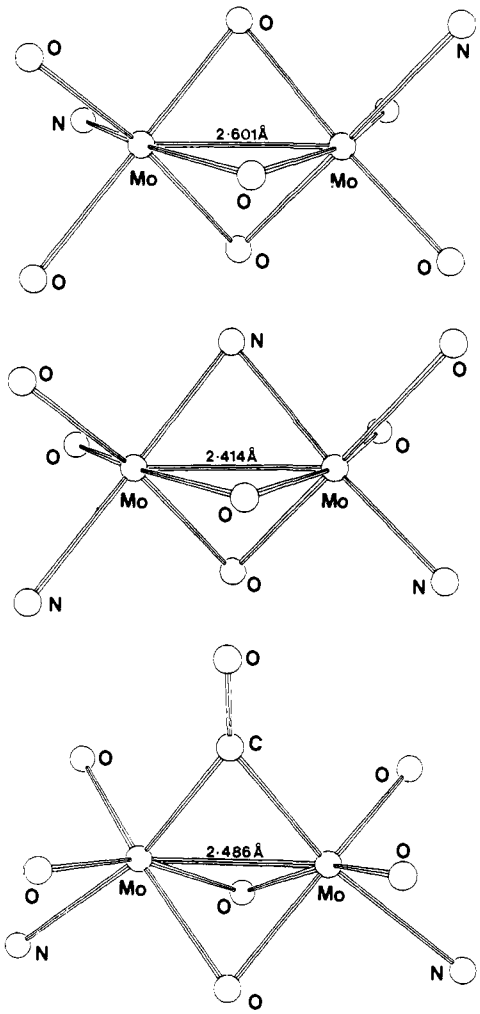

Figure 6. Comparisons of the central coordination sphere of the complexes $[Mo_2(OAr\text{-}4\text{-}Me)_7(HNMe_2)_2]^-$, $[Mo_2(OAr\text{-}3,5\text{-}Me_2)_6(NMe_2)(HNMe_2)_2]$, and $[Mo_2(O\text{-}i\text{-}Pr)_6(CO)(py)_2]$.

previous example of a complex containing an Mo_2^{7+} core has been structurally characterized for comparison. However, both $W_2Br_9^{3-}$ and $W_2Br_9^{2-}$ have been examined.[45] The effect of removing one of the electrons in the W_2^{6+} core is to increase the bond lengths from 2.41 Å in $W_2Br_9^{3-}$ to 2.60 Å in $W_2Br_9^{2-}$. We, therefore, conclude that the shorter Mo–Mo distance in $Mo_2(OAr\text{-}3,5\text{-}Me_2)_6(NMe)(HNMe_2)_2$ reflects the influence of the bridging NMe_2 group. A somewhat similar change can be seen to occur on going from a bridging Cl^- to SMe_2 in the Boorman complexes. A related complex included in Table VI is the μ-CO complex, $Mo_2(O\text{-}i\text{-}Pr)_6(py)_2(\mu\text{-}CO)$, which contains four O-*i*-Pr and two pyridine groups in terminal positions with two bridging alkoxides and one bridging CO molecule trans to the two pyridines. A comparison of the three structures is shown Figure 6. For the purposes of electron counting, the bridging CO group is normally considered as a dianion, OC^{2-}, giving a predicted Mo_2^{8+} core with the potential of forming an Mo–Mo double bond. The metal–metal distance of 2.48 Å is certainly consistent with this bonding model. Hence, the slightly shorter metal–metal distance in the μ-NMe_2, 2.41 Å, can be considered to represent a fully formed bond of order 2.5 within this geometry.

Electrochemical Behavior of $Mo_2(OAr\text{-}3,5\text{-}Me_2)_4(L)_4$ (L = $HNMe_2$; PMe_3). The use of electrochemical techniques, and in particular cyclic voltammetry, has proved to be a very useful probe to determine the electron-transfer properties of dimetal centers containing strong metal–metal interactions.[46] By successively removing or adding electons to such compounds, it is possible to vary the formal metal–metal bond order and gain insight into the stability of the resulting complexes. We have examined the electrochemistry (cyclic voltammetry, coulometry, and controlled potential electrolysis) of the two complexes $Mo_2(OAr\text{-}3,5\text{-}Me_2)_4(HNMe_2)_4$ and $Mo_2(OAr\text{-}3,5\text{-}Me_2)_4(PMe_3)_4$ by using tetrahydrofuran (THF) as solvent with $n\text{-}Bu_4N^+PF_6^-$ (TBAH; 0.2 M) as supporting electrolyte and an Ag/AgCl pseudoreference electrode. Although qualitatively similar behavior, facile oxidation, is observed for these two complexes, the ancillary neutral donor ligands have an effect on the stability of the resulting molecules.

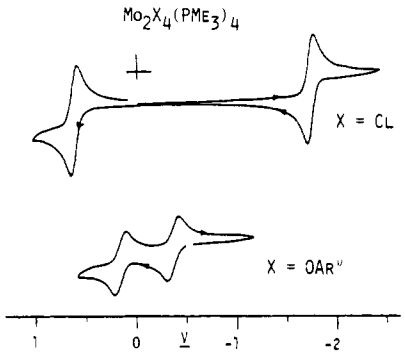

Figure 7. Comparison of the cyclic voltammogram of $Mo_2X_4(PMe_3)_4$ ($Mo\overset{4}{-}Mo$), X = Cl, OAr-3,5-Me_2.

(i) **$Mo_2(OAr\text{-}3,5\text{-}Me_2)_4(HNMe_2)_4$.** The cyclic voltammogram of blue solutions of this complex in THF/TBAH shows two, one-electron oxidation waves at −0.15 and +0.31 V vs. the Ag pseudoreference electrode. The first of these oxidation waves is pseudoreversible as judged by the presence of a reduction wave on switching the scan direction immediately after passing the first oxidation wave. The size of this reverse wave is scan-rate-dependent with $i_c/i_a \approx 1$ at rates above 450 mV/s, but $i_c/i_a < 1$ below this. Furthermore, as the scan rate is dropped, a new reduction wave begins to grow in at −0.87 V. Controlled potential oxidation at 0.0 V generates, after the passage of one electron, reddish solutions which exhibit none of the CV waves present in the parent complex. On passing through the second oxidation wave, no reverse reduction waves at all are present. We interpret these results in terms of the instability of the oxidized metal species. In particular, we believe this instability arises from the deprotonation of the cationic, dimethylamine complexes formed on oxidation. One can image that proton loss from the monocation would be slow leading to a pseudoreversible electron transfer, whereas the dication would be a considerably stronger acid and undergo a much more facile deprotonation, making electron transfer irreversible. The reduction wave at −0.87 V formed during slow CV scans may indeed be due to the presence of $[Mo_2(OAr\text{-}3,5\text{-}Me_2)_4(NMe_2)(HNMe_2)_3]$ formed by deprotonation after oxidation.

The effect of successively removing two electrons from the $Mo_2^{4+}(\sigma^2\pi^4\delta^2)$ core is to generate Mo_2^{5+} and Mo_2^{6+}p metal centers expected to contain metal–metal bonds of the order 3.5 and 3.0 with a $\sigma^2\pi^4\delta^1$ and $\sigma^2\pi^4\delta^0$ configuration, respectively. It is interesting to note that loss of two protons from the doubly oxidized species leads to $Mo_2(OAr\text{-}3,5\text{-}Me_2)_4(NMe_2)_2(HNMe_2)_2$, the species we indicated as being the possible intermediate in the $HNMe_2$ induced reduction to the Mo_2^{4+} core in the first place.

(ii) **$Mo_2(OAr\text{-}3,5\text{-}Me_2)_4(PMe_3)_4$.** Again, as with the dimethylamine complex, two one-electron oxidation waves are present in the cyclic voltammogram of the complex. However, both waves appear reversible at scan rates down to 20 mV/s with $i_a = i_c$ (Figure 7). Controlled potential oxidation at 0.0 V gen-

(42) Boorman, P. M.; Moynihan, K. J.; Oakley, R. T. *J. Chem. Soc., Chem. Commun.* **1982**, 899.
(43) Bino, A.; Cotton, F. A. *Angew. Chem., Int. Ed. Engl.* **1979**, *18*, 332.
(44) Chisholm, M. H.; Huffman, J. C.; Leonelli, J., Rothwell, I. P. *J. Am. Chem. Soc.* **1982**, *104*, 7030.
(45) Templeton, J. L.; Jacobson, R. A.; McCarley, R. E. *Inorg. Chem.* **1977**, *16*, 3320.
(46) Chisholm, M. H., Ed. *ACS Symp. Ser.* **1981**, *No. 155*, Chapter 11.

Table VII. Redox Potentials for Complexes Containing M_2^{4+} Cores (M = Mo and W)[a]

complex	$E_{1/2}$ (ox)	$E_{1/2}$ (red)	ref
$Mo_2Cl_4(PMe_2)_4$	+0.65	−1.82	this work
$Mo_2Cl_4(PBu_3)_4$[b]	+0.64	−1.92	49
$W_2Cl_4(PBu_3)_4$[b]	+0.04	−2.16	49
$Mo_2(OAr\text{-}3,5\text{-}Me_2)_4(PMe_3)_4$	−0.40, +0.24		this work
$Mo_2(OAr_3\text{-}3,5\text{-}Me_2)_4\text{-}(HNMe_2)_4$	−0.15, +0.31[c]		this work

[a] Scan rate 25 mV/s at Pt disk working electrode in THF/0.2 M TBAH in volts vs. Ag/AgCl pseudoreference electrode. [b] Scan rate 50 mV/s at Pt disk working electrode in THF/0.2 M TBAH in volts vs. SCE. [c] Irreversible oxidation, $E_{p,a}$ is quoted.

erates, after the passage of one electron, yellow-brown solutions which exhibit an identical cyclic voltammogram to the starting material except that the wave at −0.40 V is now a reduction. These solutions, therefore, contain the monocation $Mo_2(OAr\text{-}3,5\text{-}Me_2)_4(PMe_3)_4^+$ having an Mo–Mo bond of order 3.5 ($\sigma^2\pi^4\delta^1$). The second oxidation wave, despite having $i_a i_c = 1$, is not chemically reversible. Controlled potential oxidation at +0.6 V leads to deep-red solutions which have no characteristics in the CV identifiable with the parent molecule. Hence, the product of the second oxidation, the dication containing an Mo–Mo triple bond ($\sigma^2\pi^4\delta^0$), is unstable and undergoes further reactions although at a rate that is slow on the CV time scale.

The extreme ease of oxidation of the Mo_2^{4+} core in $Mo_2(OAr\text{-}3,5\text{-}Me_2)_4(PMe_3)_4$ is worthy of note. Electrochemical studies on the complexes $Mo_2Cl_4(PR_3)_4$[47] and $W_2Cl_4(PR_3)_4$[48] have been carried out by Walton et al. and Schrock et al., respectively, although the PMe_3 derivatives were not studied.

We have examined $Mo_2Cl_4(PMe_3)_4$ under our experimental conditions for comparison with the aryloxide complex (Figure 8) and included our data with certain literature data in Table VII. As expected the W_2^{4+} core is much more readily oxidized than the Mo_2^{4+} core given identical ligation, and these data have been used as a rationale for the great synthetic difficulty found in isolating $W\underline{\equiv}W$ containing species. The change in ligands from Cl to OAr-3,5-Me_2 has the effect of making the Mo_2^{4+} core much more easily oxidized, making it comparable to that of the tungsten-chloro species. Furthermore, the one-electron reduction accessible in $Mo_2Cl_4(PMe_3)_4$ is now, for the aryloxide, presumably pushed outside of the THF solvent limit. The change in ease of oxidation on going from chloro to aryloxy ancillary ligands is a characteristic change we have found for all early transition metals that we have examined. For example, the act of substitution of OAr for Cl in monomeric Ti(IV) complexes causes the complexes to become much more difficult to reduce.[49]

As mentioned previously, the one-electron oxidation of the green tetraphosphine leads to yellow-brown THF/TBAH solutions of $Mo_2(OAr\text{-}3,5\text{-}Me_2)_4(PMe_3)_4^+$ containing an odd-electron $\sigma^2\pi^4\delta^1$ metal core. The EPR spectrum of these solutions diluted with THF and cooled to −15 °C exhibit a sharp pentet with $g = 1.97$ which we assign to the unpaired electron contained in the monocation coupled to the 4-equiv ^{31}P nuclei with a coupling constant ($a = 20$ G) typical of such interactions (Figure 8). Previous studies on the oxidation of the tetrachloro analogues have only shown broad, ill-resolved signals.[48,49] The pentet shown can only be obtained on freshly prepared solutions of the monocation. Over a period of hours, the components of this multiplet change in intensity passing through a quartet pattern and eventually giving after 1 day a triplet (Figure 8). The value of the coupling constant remains 20 G, but the g value (center of pattern) shifts slightly. This change in spectral pattern is consistent with the dissociation from the Mo_2^{5+} core of one and then two PMe_3 ligands, presumably being replaced by THF molecules. The cyclic voltammogram

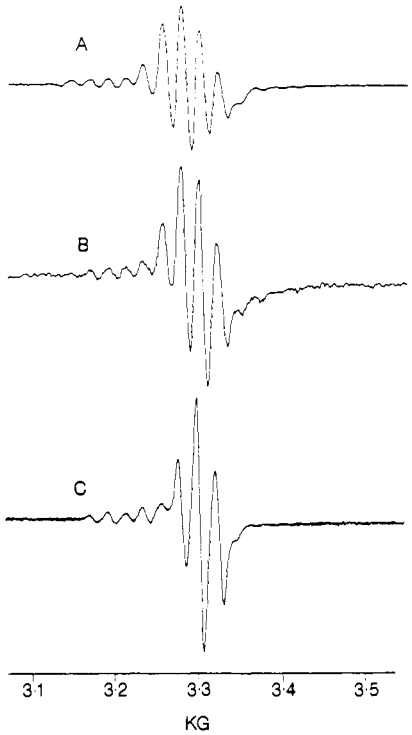

Figure 8. X-Band EPR spectra of the one-electron oxidation of $Mo_2(OAr\text{-}3,5\text{-}Me_2)_4(PMe_3)_4$ in THF/TBAH. A, initial; B, after 3 h, C, after 24 h at 25 °C.

of these "aged" solutions of the monocation do show changes with a number of new redox waves being generated close by the original monocation waves. However, the presence of a number of other broad waves indicates that other possible reactions may also be taking place.

Whether the act of oxidation to the Mo_2^{5+} core facilitates the phosphine substitution is at present unknown. Solutions of $Mo_2(OAr\text{-}3,5\text{-}Me_2)_4(PMe_3)_4$ in THF-d_8 do not dissociate free PMe_3 as determined by ^1H NMR, but only on heating at 100 °C for 24 h. However, in the absence of more controlled, quantitative experiments, the comparative rates of substitution of Mo_2^{4+} and Mo_2^{5+} cores are unknown. Unfortunately, attempts to obtain the monocation $Mo_2(OAr\text{-}3,5\text{-}Me_2)_4(PMe_3)_4^+$ in CH_2Cl_2, a noncoordinating solvent, were thwarted by a rapid reaction of green complex **8** with this solvent.

Experimental Section

All operations were performed under a dry nitrogen atmosphere either in a Vacuum Atmospheres drybox or by standard Schlenk techniques. Hydrocarbon solvents were dried by distillation from sodium benzophenone under a nitrogen atmosphere. $Mo_2(NMe_2)_6$[7], $W_2(NMe_2)_6$,[8] and $Mo_2(O\text{-}i\text{-}Pr)_6$[9] were prepared by the methods of Chisholm. Phosphines and ammines were purchased from standard sources. All phenolic reagents were purchased from Aldrich and Co. and were dried before use.

^1H and ^{31}P NMR spectra were recorded on a Varian Associates XL-200 spectrometer and are referenced to TMS or 85% H_3PO_4, respectively. Variable temperature ^1H NMR spectra were obtained by using a Perkin-Elmer R32 spectrometer (90 MHz).

$[Me_2NH_2]^+[Mo_2(OAr\text{-}4\text{-}Me)_7(HNMe_2)_2]^-\cdot n\text{-}C_6H_{14}$ (1). To a solution of $Mo_2(NMe_2)_6$ (0.700 g, 1.54 mmol) in hexane (50 mL) was added 4-methylphenol (HOAr-4-Me, 1.29 g; 12 mmol) in hexane (10 mL). The initially yellow solution became intense red on adding the phenol and was allowed to stand at room temperature. After 1 h, black crystals of product began to form, and after 12 h, the product was isolated by decanting off the mother liquor and washing the product with hexane: yield 85%. Anal. Calcd for $C_{61}H_{85}N_3O_2Mo_2$: C, 62.93; H, 7.36; N, 3.61. Found: C, 62.50; H, 7.30; N, 3.62. ^1H NMR (C_6D_6, 30 °C) δ 5.10, 5.40, 5.57, 5.75 (in ratio of 2:2:1:2 due to 4-methylphenoxy resonances).

$[Me_2NH_2]^+[Mo_2(OAr\text{-}3,5\text{-}Me_2)_7(HNMe_2)_2]^-$ (2). When a similar procedure to that for the 4-methylphenol complex (**1**) was used except using 3,5-dimethylphenol (HOAr-3,5-Me_2), dark crystals of **2** could be obtained in yields up to 65%. Anal. Calcd for $C_{62}H_{85}N_3O_7Mo_2$: C, 63.31; H, 7.28; N, 3.57. Found: C, 63.32; 7.37; N, 3.74.

(47) Zietlow, T. C; Kledworth, D. D.; Nimry, T.; Salmon, D. J.; Walton, R. A. *Inorg. Chem.* **1981**, *20*, 947.
(48) Schrock, R. R.; Sturgeoff, L. G.; Sharp, P. R. *Inorg. Chem.* **19838** *22*, 2801.
(49) Durfee, L.; Latesky, S.; Rothwell, I. P., unpublished results.

Mo_2(OAr-3,5-Me_2)$_6$ (3). Addition of 3,5-dimethylphenol (HOAr-3,5-Me_2, 6 equiv) to hexane solutions of Mo_2(O-i-Pr)$_6$ gave a deep-red solution which on removal of solvent and generated isopropyl alcohol gave the product as a red powder in almost quantitative yield. Anal. Calcd for $C_{48}H_{54}O_6Mo_2$: C, 62.74; H, 5.92. Found: C, 63.05; H, 6.19. ^{1}H NMR (C_6D_6, 30 °C) δ 2.05 (s, 3.5-Me_2), 6.21 (s, ortho-H), 6.42 (s, para-H).

Mo_2(OAr-4-F)$_6$(HNMe$_2$)$_2$ (4). Addition of 4-fluorophenol (HOAr-4-F, 7 equiv) to hexane solutions of Mo_2(NMe$_2$)$_6$ gave a deep-red mixture which on standing rapidly precipitated out the product as a deep-red solid which was washed with hexane. The yield was greater than 95%. Anal. Calcd for $C_{40}H_{38}F_6O_6N_2Mo_2$: C, 50.43; H, 3.82; N, 2.94. Found: C, 50.19; H, 4.06; N, 3.06. ^{1}H NMR (C_6D_6, 30 °C) δ 1.85 (d, HN*Me*$_2$), 4.28 (m, *H*NMe$_2$), 6.2–6.9 (m, aromatics).

W_2(OAr-4-Me)$_6$(HNMe$_2$)$_2$ (5). Using an identical procedure to that used to prepare 4 only using W_2(NMe$_2$)$_6$ and 4-methylphenol gave the product **5** as a yellow–brown solid. ^{1}H NMR (C_6D_6, 30 °C) δ 2.10 (s, OAr-4-Me, cis to HNMe$_2$), 2.29 (s, OAr-4-Me, trans to HNMe$_2$), 2.20 (d, HN*Me*$_2$), 6.9–7.4 (*H*NMe$_2$ and aromatics).

W_2(OAr-3,5-Me_2)$_6$(HNMe$_2$) (6). Using 3,5-dimethylphenol instead of 4-methylphenol gave **6** as yellow crystals. Anal. Calcd for $C_{52}H_{68}N_2O_6W_2$: C, 52.71; H, 5.79; N, 2.36. Found: C, 53.01; H, 5.82; N, 2.31. ^{1}H NMR (C_6D_6, 30 °C) δ 2.27 (s, OAr-3,5-*Me*$_2$, cis to HNMe$_2$), 2.32 (s, OAr, 3.5-*Me*$_2$, trans to HNMe$_2$), 2.38 (d, HN*Me*$_2$), 4.87 (septet, *H*NMe$_2$), 6.5–7.1 (m, aromatics).

Mo_2(OAr-3,5-Me_2)$_4$(HNMe$_2$)$_4$ (7). To a yellow hexane (25 mL) solution of Mo_2(NMe$_2$)$_6$ (1.00 g) was aded 3,5-dimethylphenol (4.5 equiv). Into the resulting deep-red mixture was then condensed 10 mL of HNMe$_2$ at liquid nitrogen temperatures. The solution was allowed to warm up to room temperature (CAUTION: A positive pressure of HNMe$_2$ gas may develop. The mixture was kept in a robust flask fitted with a Kontes Teflon valve). After 20 h, the deep-blue crystalline precipitate of product **7** was isolated by decanting off the deep-red hexane/HNMe$_2$ mother liquor under N_2 and washing with hexane: yield 67%. Anal. Cald for $C_{40}H_{64}N_4O_4Mo_2$: C, 56.04; H, 7.53; N, 6.54. Found: C, 56.20; H, 7.31; N, 6.30. ^{1}H NMR (C_6D_6, 30 °C) δ 2.34 (s, 3,5-*Me*$_2$), 2.64 (d, HN*Me*$_2$), 6.59 (m, *H*NMe$_2$); 5.96 (s, *o-H*); 6.45 (s, *p-H*). The infrared spectrum as a Nujol mull shows $\nu_{(N-H)}$ at 3095 cm^{-1} (br).

Mo_2(OAr-3,5-Me_2)$_4$(PMe$_3$)$_4$ (8). A blue solution of Mo_2(OAr-3,5-Me_2)$_4$(HNMe$_2$)$_4$ (**7**) in neat excess PMe$_3$ was sealed into an evacuated tube at liquid N_2 temperatures. The tube was then gently heated at 50 °C for 20 h to give a deep-green solution. The tube was opened, and the HNMe$_2$ and excess PMe$_3$ were removed under vacuum to give emerald crystals of product. Anal. Calcd for $C_{44}H_{72}O_4P_4Mo_2$: C, 53.88; H, 7.40; P, 12.63. Found: C, 54.04; H, 7.49; P, 12.41. ^{1}H NMR (C_6D_6, 30 °C) δ 1.37 (br, P*Me*$_3$), 2.27 (s, 3,5-*Me*$_2$), 5.93 (s, *o-H*), 6.37 (s, *p-H*). ^{31}P NMR (benzene, 30 °C) δ −9.87 (s) vs 85% < H_3PO_4.

Electrochemical Measurements. Cyclic voltammograms were obtained by using a BioAnalytical Systems, Inc., Model CV-1A instrument. Potential control for coulometric experiments was performed with a potentiostat purchased from Bio-Analytical Systems, Inc. A three-compartment (H) cell was used with a Pt disk or gauze working electrode, Pt wire auxiliary electrode, and Ag/AgCl pseudoreference electrode[50] to which all potentials refer. Scan rates were 25 mV/s. Under these conditions, the Cp_2Fe/Cp_2Fe^+ couple was measured at +0.47 V consistent to ±10 mV, with a separation between the anodic and cathodic waves of 90 mV.

X-ray Crystallography. The two structures contained in this paper were determined in different laboratories, the first at Indiana University and the second at Purdue University. This is reflected in the crystallographic data contained in Table I.

[Me_2NH_2][Mo_2(OAr-4-Me)$_7$(HNMe$_2$)$_2$]·*n*-C_6H_{14} (1). General operating procedures have been previously described.[50] A suitable fragment of the compound was cleaved from a larger clump of well-formed crystals and transferred to the goniostat by using standard inert atmosphere handling techniques employed by the IUMSC. All data were collected at −169 °C by using a gas flow cooling system.

A systematic search of a limited hemisphere of reciprocal space revealed no systematic extinctions or symmetry, leading to the assignment of a triclinic space group. Subsequent solution and refinement confirmed the space group to be *P*1 bar.

The structure was solved by a combination of direct methods and Patterson and Fourier techniques. All atoms were located and refined anisotropically. While some hydrogen atoms were visible in the difference Fourier phased on the non-hydrogen parameters, the data were not of sufficient resolution to allow their refinement. For this reason, hydrogen atoms were included as fixed atom contributor for all atoms except for the methyl hydrogens on the paramethyltolyl groups.

A final difference map was featureless, with peaks of up to 0.65 e/A^3 scattered throughout the unit cell. While several were in logical positions to be identified as the missing methyl hydrogens, it was not considered practical to include them.

Psi scans for several reflections indicated that no absorption correction was necessary.

Mo_2(OAr-3,5-Me_2)$_6$(NMe$_2$)(HNMe$_2$)$_2$ (9). Dark-blue, block-shaped crystal of the complex was mounted on a glass fiber in a random orientation. Preliminary examination and data collection were performed with Mo Kα radiation (λ = 0.71073 Å) on an Enraf-Nonius CAD4 computer-controlled κ axis diffractometer equipped with a graphite crystal, incident beam monochromator. Cell constants and an orientation matrix for data collection were obtained from least-squares refinement, using the setting angles of 24 reflections in the range 35 < 2θ < 36, measured by the computer-controlled diagonal slit method of centering. As a check on crystal quality, ω scans of several intense reflections were measured; the width at half-height was 0.40 with a take-off angle of 5.0, indicating moderate crystal quality. From the systematic absence of

$$h01 \quad h + 1 = 2n + 1$$

$$0k0 \quad k = 2n + 1$$

and for subsequent least-squares refinement, the space group was determined to be $P2_1/n$.

The data were collected at a temperature of −140 (2) °C by using the ω − 2θ scan technique. The scan rate varied from 2 to 3 deg/min (in ω). The variable scan rate allows rapid data collection for intense reflections where a fast scan rate is used and assures good counting statistics for weak reflections where a slow scan rate is used. Data were collected to a maximum 2θ of 50.0°. The scane range (in deg) was determined as a function of θ to correct for the separation of the Kα doublet; the scan width was calculated as follows:

$$\omega \text{ scan width} = 0.9 + 0.200 \tan\theta$$

Moving-crystal moving-counter background counts were made by scanning an additional 25% above and below this range. Thus, the ratio of peak counting time to background counting time was 2:1. The counter aperture was also adjusted as a function of θ. The horizontal aperture width ranged from 3.8 to 4.2 mm; the vertical aperture was set at 4.0 mm. The diameter of the incident beam collimator was 0.7 mm, and the crystal to detector distance was 21 cm. For intense reflections, an attenuator was automatically inserted in front of the detector; the attenuator factor was 25.7.

A total of 9113 reflections were collected, of which 9106 were unique and not systematically absent. As a check on crystal and electronic stability, three representative reflections, (−6,8,1), (11,3,6), (−7,3,10), were measured every 120 min. The intensities of these standards remained constant within experimental error throughout data collection. No decay correction was applied.

Lorentz and polarization corrections were applied to the data. The linear absorption coefficient is 5.2 cm^{-1} for Mo Kα radiation. No absorption correction was made. The structure was solved by direct methods. When 440 reflections (minimum *E* of 1.56) and 9788 relationships were used, a total of 32 phase sets were produced. A total of 16 atoms were located from an *E* map prepared from the phase set with probability statistics; absolute figure of merit = 1.178, residual = 9.32, and psi zero = 3.422. The remaining atoms were located in succeeding difference Fourier synthesis. Hydrogen atoms were located and added to the structure factor calculations but their positions were not refined. The structure was refined by using modified block diagonal least squares where the function minimized as $\sum w(|F_o| - F_c|)^2$ and the weight *w* is defined as $4F_o^2/\sigma^2(F_o^2)$.

The standard deviation on intensities, $\sigma(F_o^2)$, is defined as

$$\sigma^2(F_o^2) = [S^2(C + R^2B) + (pF_o^2)^2]/L_p^2$$

where *S* is the scan rate, *C* is the total integral peak count, *R* is the ratio of scan time to background counting time, *B* is the total background count, L_p is the Lorentz polarization factor, and the parameter *p* is a factor introduced to downweight intense reflections. Here *p* was set to 0.040. The final cycle of refinement included 586 variable parameters and converged (largest parameter shift was 0.06 times is esd) with unweighted and weighted agreement factors of

$$R1 = \sum||F_c| - |F_c||/\sum|F_o| = 0.053$$

$$R2 = SQRT(\sum w(|F_o| - |F_c|)^2/\sum wF_o^2) = 0.059$$

The standard deviation of an observation of unit weight was 0.89. The highest peak in the final difference Fourier had a height of 1.38 e/A^3

(50) Huffman, J. C.; Lewis, L. N.; Caulton, K. G. *Inorg. Chem.* **1980**, *19*, 2755.

with an estimated error bsed on F of 0.13. Plots of $\sum w(|F_0| - |F_c|)^2$ vs. $|F_0|$, reflection order in data collection, sin θ/λ, and various classes of indexes showed no unusual trends.

Acknowledgment. We thank the National Science Foundation (Grant CHE-8219206 to I.P.R.) for financial support of this work and Amoco for a fellowship (to T.W.C.). We also thank the Monsanto Fund and the National Science Foundation for Financial support of the X-ray facilities at Purdue University.

Supplementary Material Available: Complete listings on bond lengths and bond angles, anisotropic thermal parameters, structure factors, and calculated fittings of the observed temperature dependence of the 4-methyl groups of the salt complex to values of δ and J (105 pages). Ordering information given on any current masthead page.

Tungsten as a Weak Backscatterer: An Example of Information Loss in Extended X-ray Absorption Fine Structure (EXAFS) Spectroscopy. Tungsten and Iron EXAFS Studies of Tungsten–Iron–Sulfur Clusters Containing the WS_2Fe Unit

Mark R. Antonio,[1a,b] Boon K. Teo,*[1c] and Bruce A. Averill*[1a,d]

Contribution from AT&T Bell Laboratories, Murray Hill, New Jersey 07974, Department of Chemistry, Michigan State University, East Lansing, Michigan 48824, and Department of Chemistry, University of Virginia, Charlottesville, Virginia 22901. *Received June 11, 1984*

Abstract: The W L_3-edge and Fe K-edge transmission EXAFS (extended X-ray absorption fine structure) spectra of the binuclear complex ions $[S_2WS_2FeX_2]^{2-}$ (**1**, X = SPh; **2**, X = Cl, **3**, X = OPh; Et_4N^+ salts; and **4**, $X_2 = S_5$; Ph_4P^+ salt), the trinuclear complex ions $[S_2WS_2FeS_2Fe(S\text{-}p\text{-}C_6H_4CH_3)_2]^{3-}$ (**5**, Et_4N^+ salt) and $[Cl_2FeS_2WS_2FeCl_2]^{2-}$ (**6**, Ph_4P^+ salt), and the W L_3-edge transmission EXAFS spectrum of tetrathiotungstate, $[WS_4]^{2-}$ (**7**, NH_4^+ salt), have been measured and interpreted. The structural parameters and parameter correlation curves obtained from the FABM (fine adjustment based on models) analysis of the W and Fe EXAFS data for the WS_2Fe complex anions (**1–6**, this work) closely parallel those from the FABM analysis of the Mo and Fe EXAFS data for the MoS_2Fe cluster anion analogues. An important aspect of the present study is the near-absence of the Fe–W peak in the Fourier transforms of the Fe EXAFS data for **1–6**. This represents a type of *information loss* in EXAFS spectroscopy and points to the fact that, in sharp contrast to the principles of X-ray diffraction, the general assumption that heavier elements are stronger backscatterers than lighter ones does not always hold true in EXAFS spectroscopy. This observation is explained in terms of the shape of the W backscattering amplitude profile; there are two minima in the W backscattering amplitude function at ca. 5 and 10 Å^{-1} over the photoelectron wavevector (k) range of practical importance ($3 \lesssim k \lesssim 15$ Å^{-1}). For systems that contain tungsten neighbors in the vicinity of the X-ray absorbing atom, the tungsten peak may be enhanced by extending the data out to high k values ($k > 15$ Å^{-1}) and/or by reducing the Debye–Waller factor by data collection at low temperatures. It is suggested that weak EXAFS backscatterers be avoided in heavy-atom substitution studies, especially for dilute biological systems.

Although the chemistry of synthetic metal–sulfur clusters of the group 6 transition elements molybdenum and tungsten is similar, significant differences are observed when nitrogenase-producing organisms are grown on tungstate in place of molybdate.[2,3] Growth under such conditions renders the nitrogenase system extremely unstable and nonfunctional for the reduction of dinitrogen.[2,3] The putative WFe analogue of the MoFe protein of nitrogenase is presumably either unstable or possesses properties that are incompatible with the function of the metalloenzyme. In view of the inability of tungsten to participate in a functional nitrogenase, the tungsten analogues of several synthetic Mo–Fe–S cluster anions containing the $MoFe_3S_4$ cubane core and the MoS_2Fe core have been prepared and characterized.[4-7] Comparisons of the properties and structures of W–Fe–S clusters containing the WFe_3S_4 and WS_2Fe units to those of the corresponding Mo–Fe–S clusters containing the $MoFe_3S_4$ and MoS_2Fe units (which represent potential structural fragments of the MoFe protein and FeMo cofactor of nitrogenase) are thus of appreciable interest. We report here the results of the W L_3-edge and Fe K-edge transmission EXAFS (extended X-ray absorption fine structure) studies of binuclear complex ions $[S_2WS_2FeX_2]^{2-}$ (**1**, X = SPh,[8a,b] **2**, X = Cl;[7,8a,c,9] **3**, X = OPh;[8a,b] Et_4N^+ salts; and

Chart I

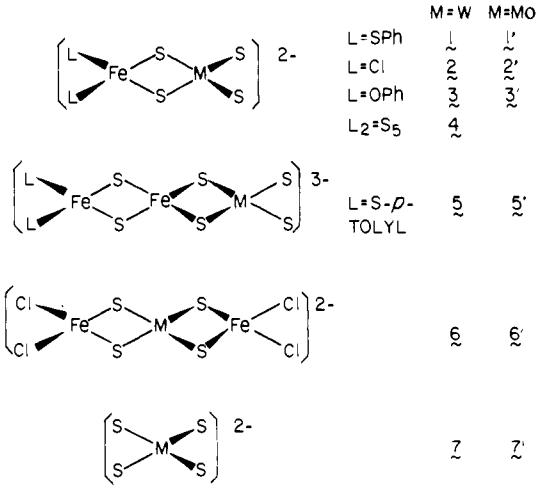

(1) (a) Michigan State University, Department of Chemistry, East Lansing, Michigan 48824. (b) Current address: The Standard Oil Company (Ohio), Warrensville Research Center, Cleveland, Ohio 44128. (c) AT&T Bell Laboratories, Murray Hill, New Jersey 07974. (d) Current address: University of Virginia, Department of Chemistry, Charlottesville, Virginia 22901.

(2) Benemann, J. R.; Smith, G. M.; Kostel, P. J.; McKenna, C. E. *FEBS Lett.* **1973**, *29*, 219.
(3) Nagatani, H. H.; Brill, W. J. *Biochim. Biophys. Acta* **1974**, *362*, 160.
(4) Averill, B. A. *Struct. Bonding (Berlin)* **1983**, *53*, 59.
(5) Holm, R. H. *Chem. Soc. Rev.* **1981**, *10*, 455.
(6) Müller, A.; Diemann, E.; Jostes, R.; Bögge, H. *Angew. Chem., Int. Ed. Engl.* **1981**, *20*, 934.
(7) Coucouvanis, D. *Acc. Chem. Res.* **1981**, *14*, 201.

0002-7863/85/1507-3583$01.50/0 © 1985 American Chemical Society